Introduction to Climate

Tomoaki OSE (MRI/JMA)

Climate Research Department
Meteorological Research Institute (MRI/JMA)

Climate and Climate System

"Weather is what is happening to the atmosphere at any given time.

Climate in a narrow sense is the "average weather," the statistical description over a period of time."

Climate is formed in the interactions in climate system, consisting of atmosphere including composition and circulation, the ocean, hydrosphere, land surface, biosphere, snow and ice, solar and volcanic activities in its spatial and temporal variability.

Climate System

http://ipcc-wg1.ucar.edu/wg1/FAQ/wg1_faq-1.2.html

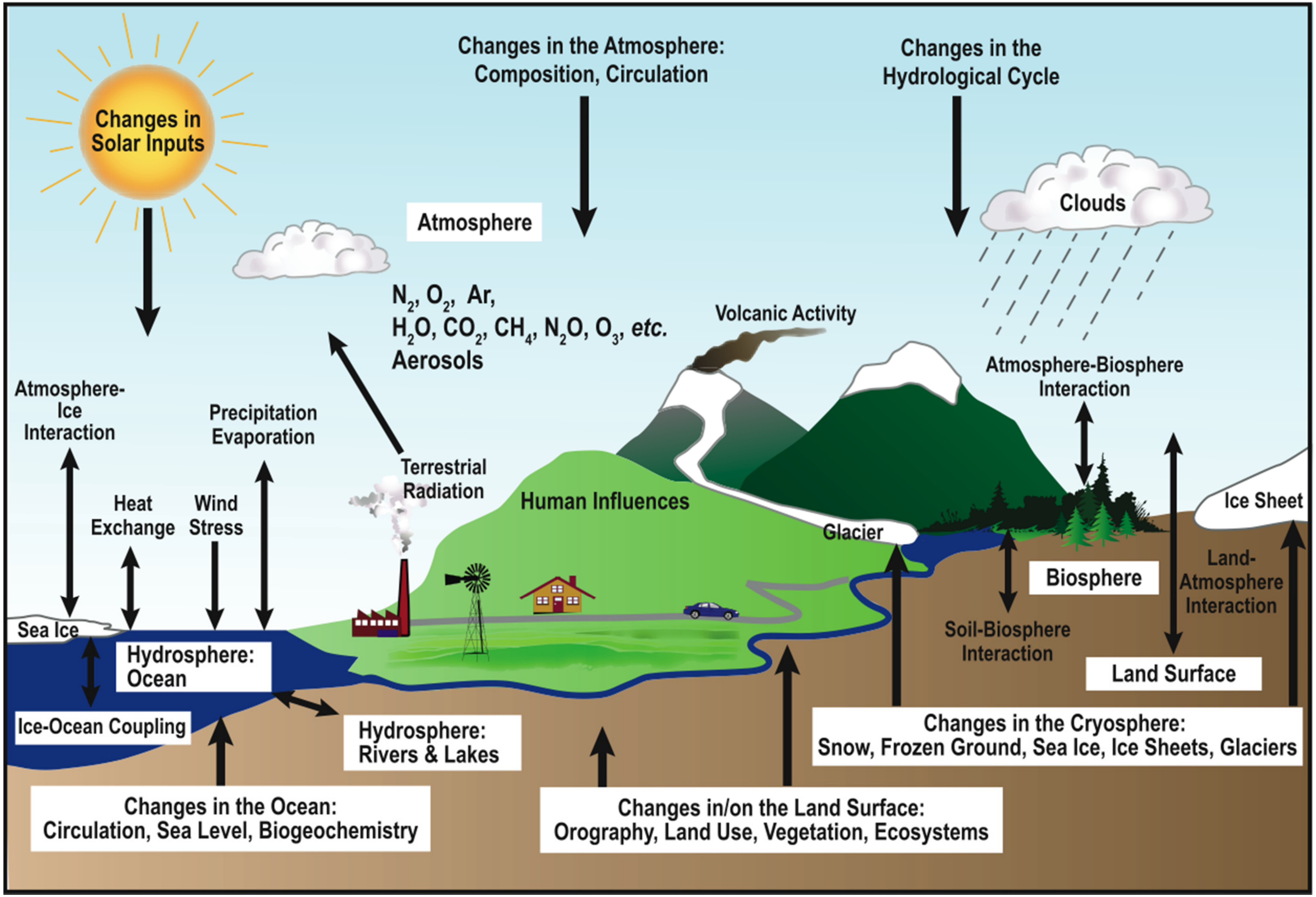

Schematic view of the components of the climate system, their processes and interactions.

Radiative Balance

Radiative Balance between Earth and Space

- **Solar Radiation**
  - Solar constant : $S \approx 1370\ Wm^{-2}$
  - insolation : $\frac{S}{4} \approx 342 Wm^{-2}$
  - planetary albedo : $\alpha_P \approx 0.31$
  - absorption : $\frac{S}{4}(1-\alpha_P) \approx 235 Wm^{-2}$
- **Terrestrial Radiation**
  - equilibrium radiative temperature : T_e^*
  - emission : σT_e^{*4}

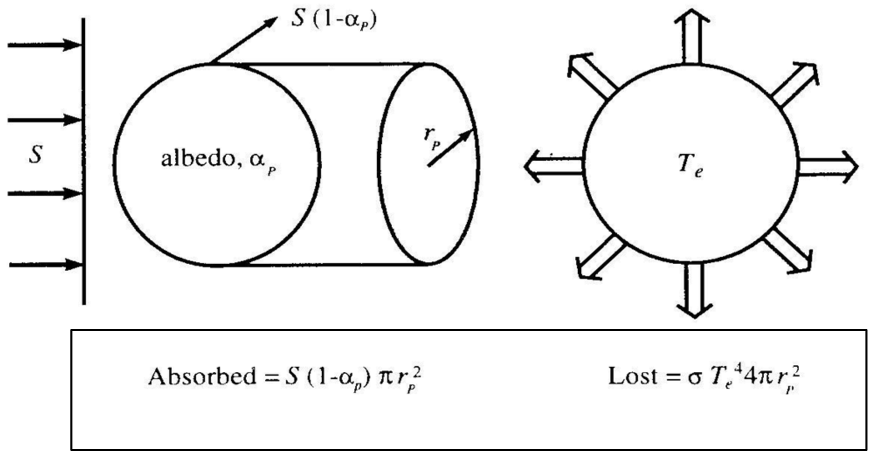

- **Radiation Balance**
  - Balance between absorbed solar radiation and terresitrial emission

$$T_e^* = \sqrt[4]{\frac{S(1-\alpha_P)}{4\sigma}} \approx 254\,K \approx -19°C$$

Earth's temperature observed from the cosmic space

Surface Temperature = 15° C

Pictures are from NASA web-sites

Difference between
Equilibrium radiative temperature and Ground Surface Temperature

Venus

- **Solar constant : 2600 W/m2**
- **planetary albedo : 0.77**
- **Equilibrium radiative temperature : - 46° C**

Earth

- **Solar constant :** $S \approx 1370\ Wm^{-2}$
- **planetary albedo :** $\alpha_P \approx 0.31$
- **Equilibrium radiative temperature**

$$T_e^* = \sqrt[4]{\frac{S(1-\alpha_P)}{4\sigma}} \approx 254\,K \approx -19°C$$

Mars

- **Solar constant : 590 W/m2**
- **planetary albedo : 0.15**
- **Equilibrium radiative temperature : -56° C**

Surface Temperature

457° C

Surface Pressure

90,000hPa

Surface Temperature

15° C

Surface Pressure

1,000hPa

Surface Temperature

-55° C

Surface Pressure

10hPa

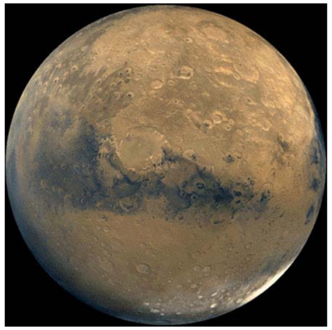

http://ipcc-wg1.ucar.edu/wg1/FAQ/wg1_faq-1.1.html

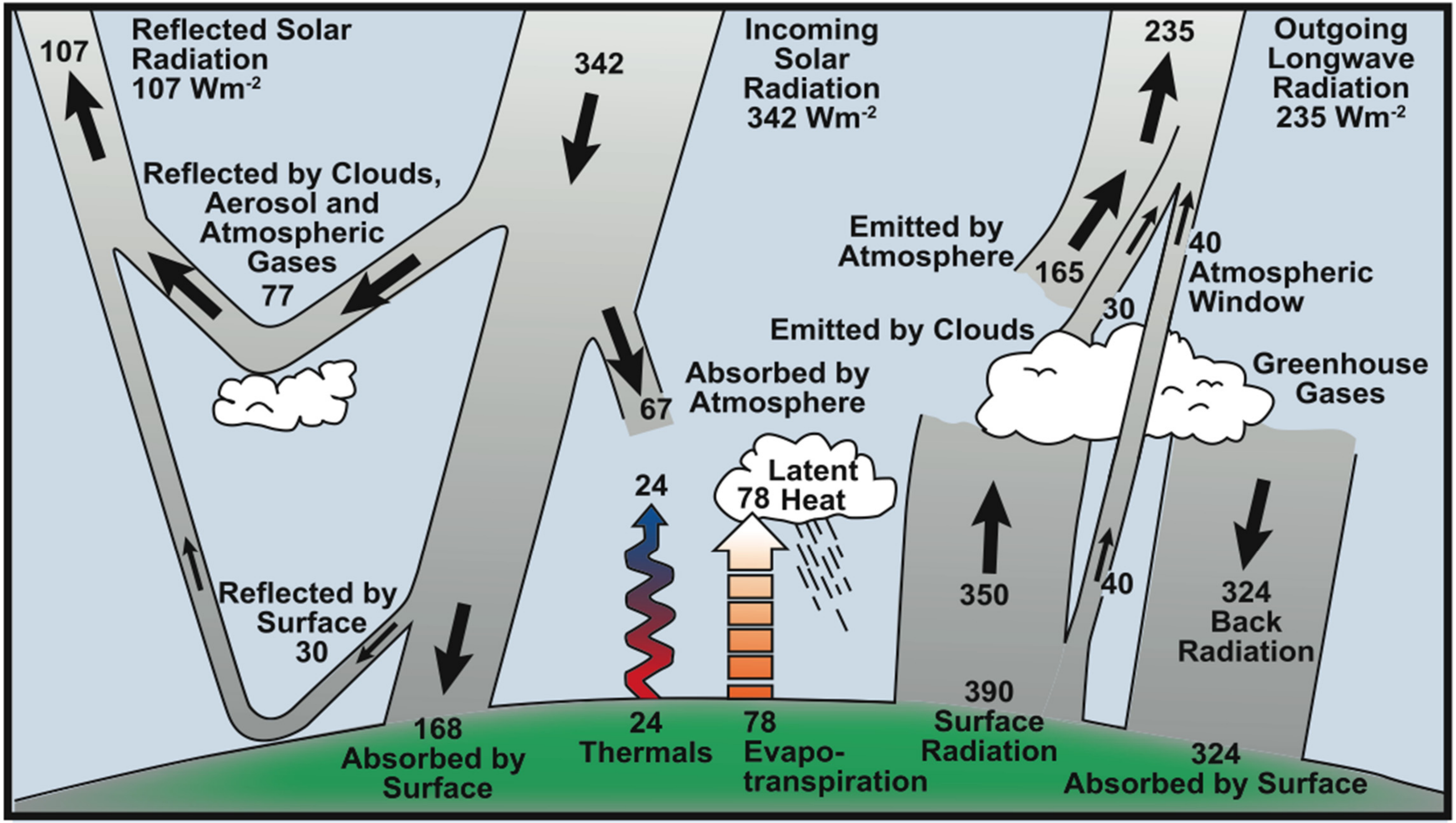

Estimate of the Earth's annual and global mean energy balance. Over the long term, the amount of incoming solar radiation absorbed by the Earth and atmosphere is balanced by the Earth and atmosphere releasing the same amount of outgoing longwave radiation. About half of the incoming solar radiation is absorbed by the Earth's surface. This energy is transferred to the atmosphere by warming the air in contact with the surface (thermals), by evapotranspiration and by longwave radiation that is absorbed by clouds and greenhouse gases. The atmosphere in turn radiates longwave energy back to Earth as well as out to space. Source: Kiehl and Trenberth (1997).

http://ipcc-wg1.ucar.edu/wg1/FAQ/wg1_faq-1.1.html

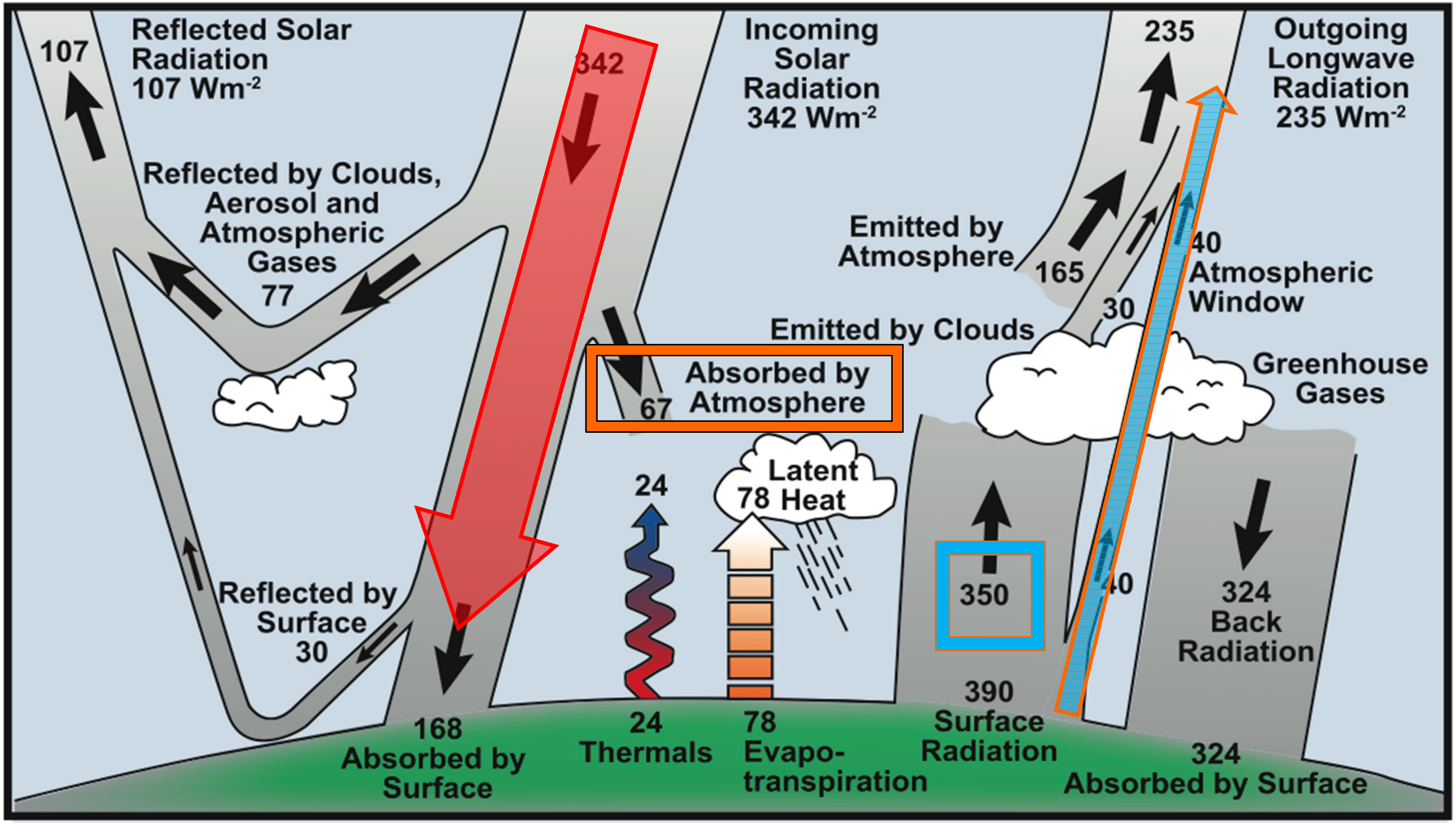

Estimate of the Earth's annual and global mean energy balance. Over the long term, the amount of incoming solar radiation absorbed by the Earth and atmosphere is balanced by the Earth and atmosphere releasing the same amount of outgoing longwave radiation. About half of the incoming solar radiation is absorbed by the Earth's surface. This energy is transferred to the atmosphere by warming the air in contact with the surface (thermals), by evapotranspiration and by longwave radiation that is absorbed by clouds and greenhouse gases. The atmosphere in turn radiates longwave energy back to Earth as well as out to space. Source: Kiehl and Trenberth (1997).

Pictures are from NASA and JMA web-sites

Absorption of Radiation from 6000K and 255K Blackbodies

Solar radiation

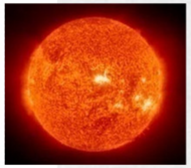

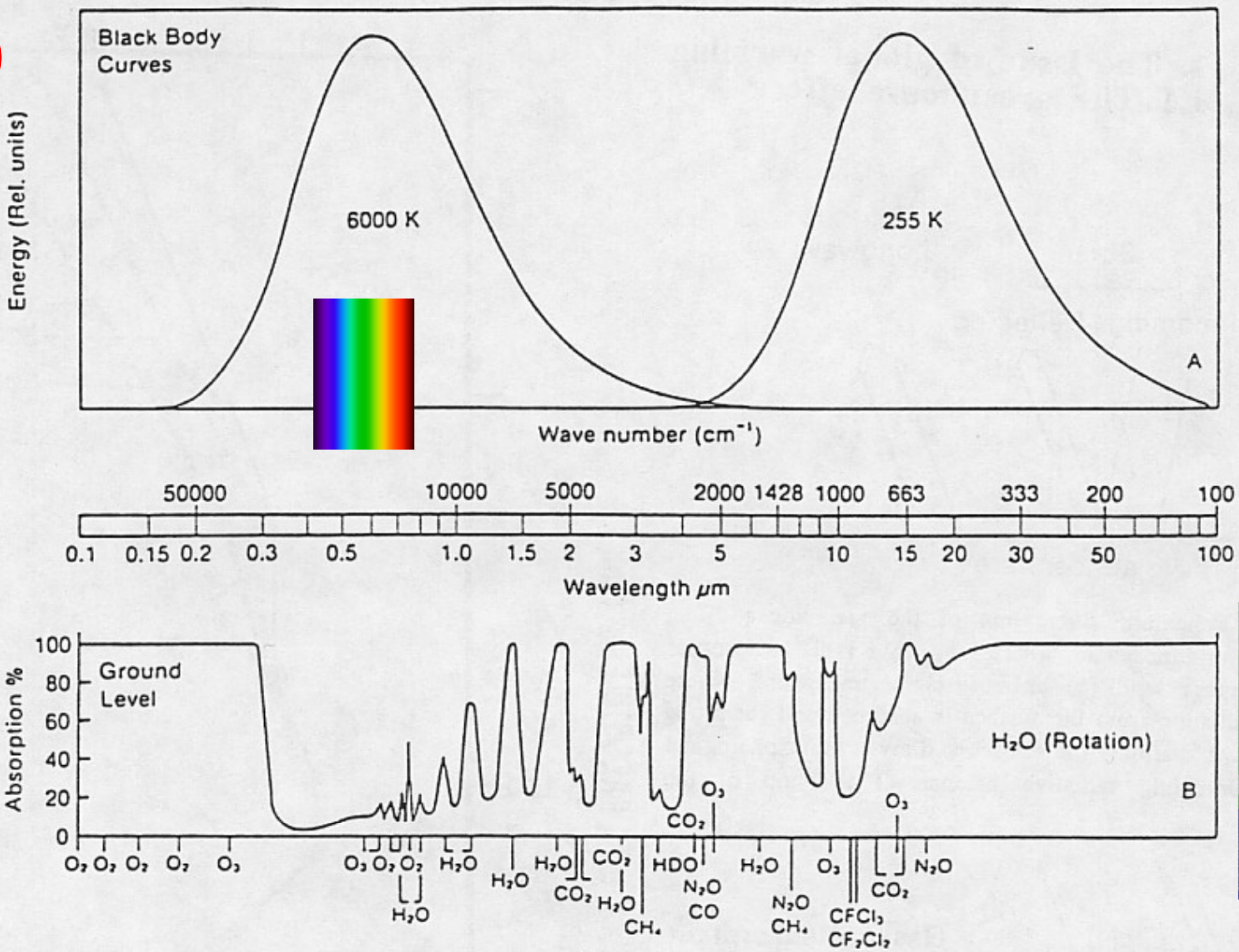

Terrestrial radiation

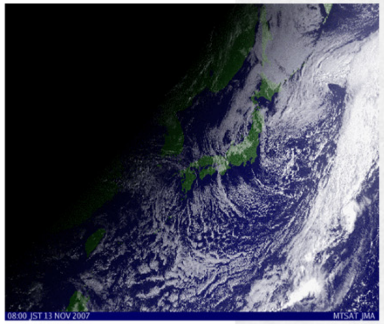

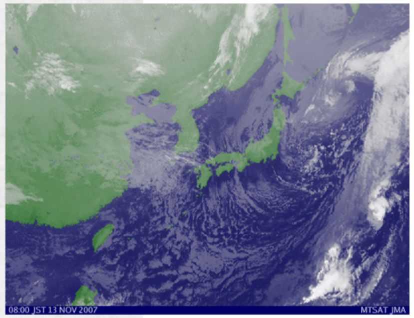

(*a*) Spectral distribution of long-wave emission from blackbodies at 6000 K and 255 K, corresponding to the mean emitting temperatures of the Sun and Earth, respectively, and (*b*) percentage of atmospheric absorption for radiation passing from the top of the atmosphere to the surface. Notice the comparatively weak absorption of the solar spectrum and the region of weak absorption from 8 to 12 μm in the long-wave spectrum [from *MacCracken and Luther*, 1985].

Radiative heating tends to create vertical instability

between heated ground and cooled atmosphere on average

http://ipcc-wg1.ucar.edu/wg1/FAQ/wg1_faq-1.1.html

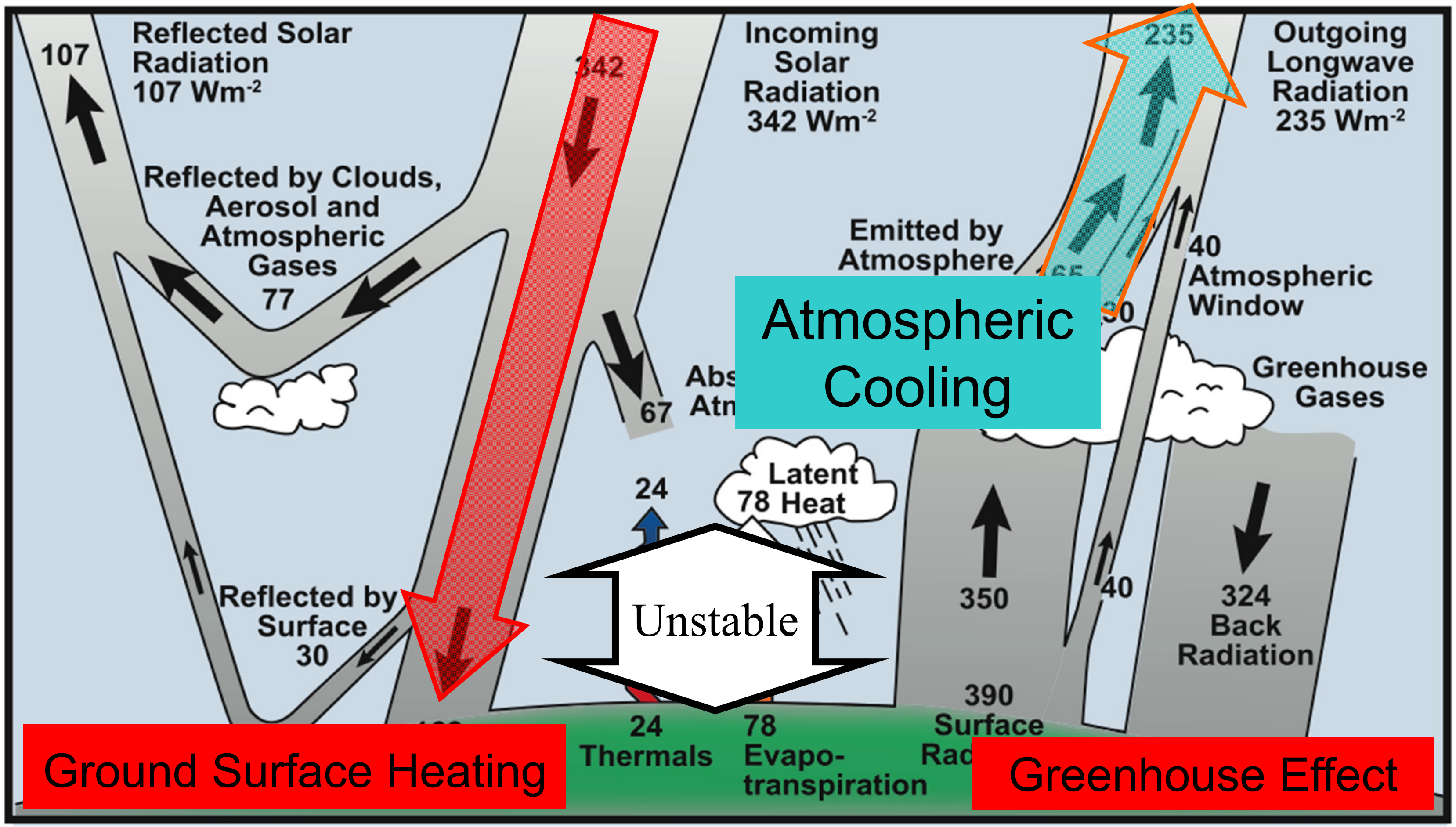

Estimate of the Earth's annual and global mean energy balance. Over the long term, the amount of incoming solar radiation absorbed by the Earth and atmosphere is balanced by the Earth and atmosphere releasing the same amount of outgoing longwave radiation. About half of the incoming solar radiation is absorbed by the Earth's surface. This energy is transferred to the atmosphere by warming the air in contact with the surface (thermals), by evapotranspiration and by longwave radiation that is absorbed by clouds and greenhouse gases. The atmosphere in turn radiates longwave energy back to Earth as well as out to space. Source: Kiehl and Trenberth (1997).

One-Dimensional
Vertical Profile Model

Thermal Equilibrium of the Atmosphere with a Convective Adjustment

Syukuro Manabe and Robert F. Strickler

General Circulation Research Laboratory, U. S. Weather Bureau, Washington, D. C.

(Manuscript received 19 December 1963, in revised form 13 April 1964)

Typical condition at 35N in April

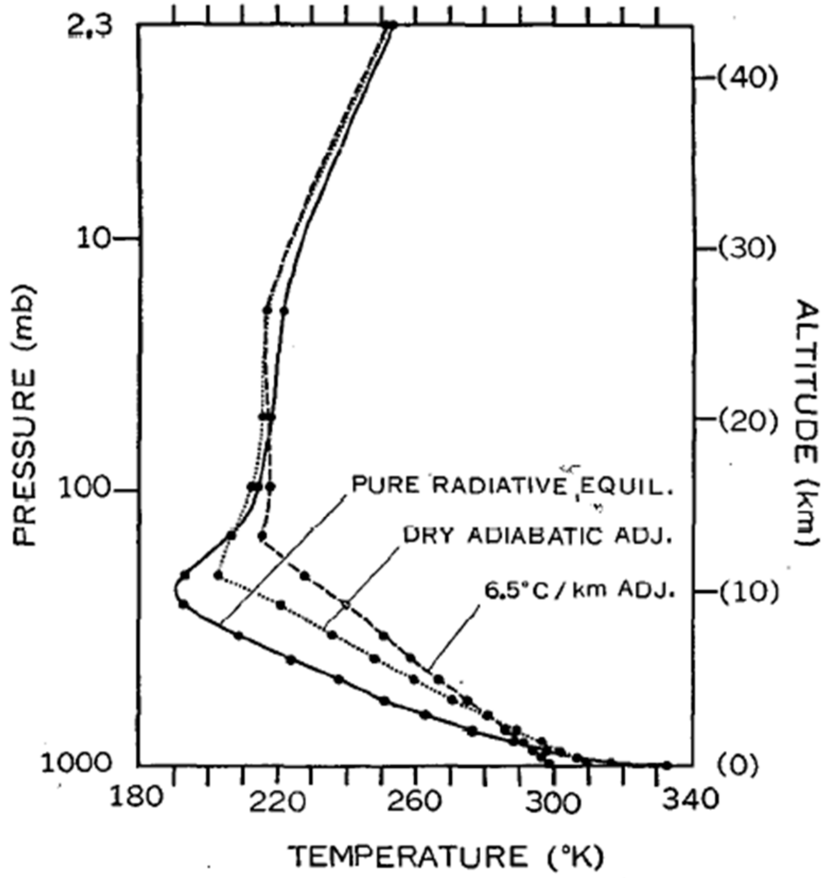

Fig. 4. The dashed, dotted, and solid lines show the thermal equilibrium with a critical lapse rate of 6.5 deg km^{-1}, a dry-adiabatic critical lapse rate (10 deg km^{-1}), and pure radiative equilibrium.

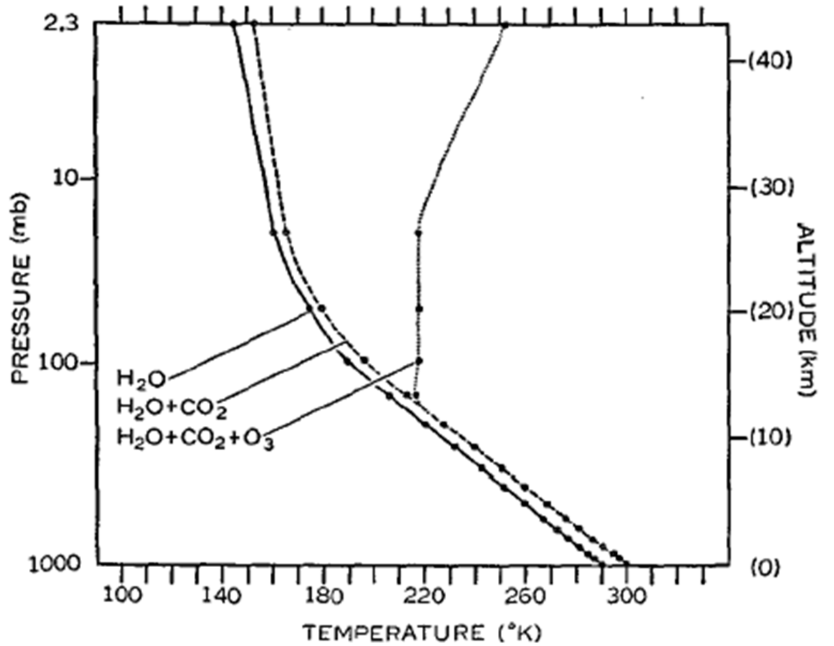

Fig. 6c. Thermal equilibrium of various atmospheres which have a critical lapse rate of 6.5 deg km^{-1}. Vertical distributions of gaseous absorbers at 35N, April, were used. $S_c=2$ ly min^{-1}, $\cos\bar{\zeta}=0.5$, $r=0.5$, no clouds.

One-Dimensional Vertical Profile Model

Thermal Equilibrium of the Atmosphere with a Convective Adjustment

SYUKURO MANABE AND ROBERT F. STRICKLER

General Circulation Research Laboratory, U. S. Weather Bureau, Washington, D. C.

(Manuscript received 19 December 1963, in revised form 13 April 1964)

Observed Temperature

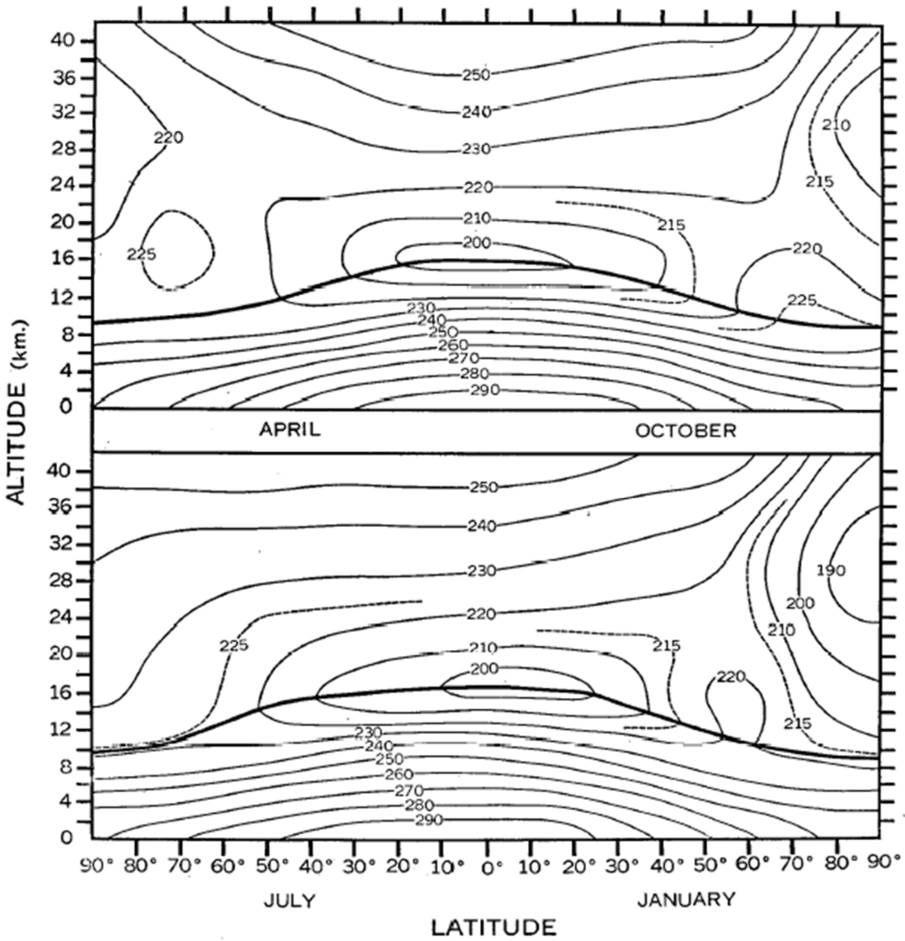

FIG. 12. Distribution of the observed temperature (deg k) in the northern hemisphere for different seasons. From J. London (1956).

1-D model Simulations for each latitudes

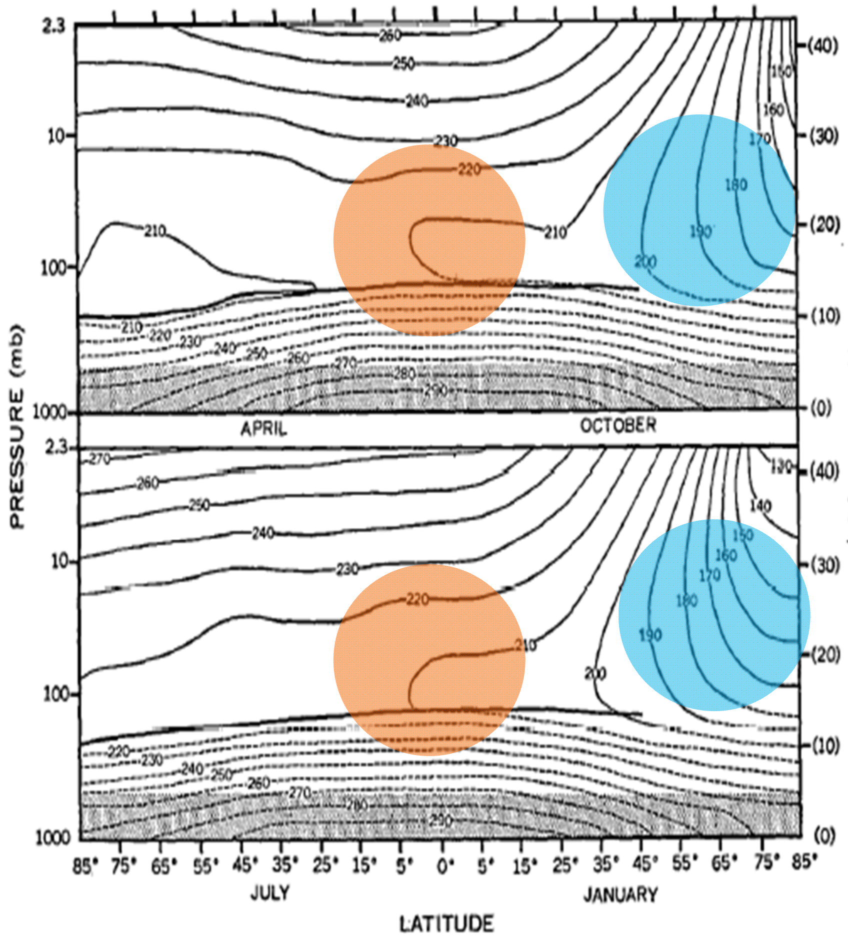

FIG. 13. The local radiative equilibrium temperature of the stratosphere. The shaded area is the region where the temperature was fixed at the observed value. Above the shaded area the state of the convective equilibrium, whose critical lapse rate for convective adjustment is deg km⁻¹, is shown. The region covered by solid lines is in local radiative equilibrium.

Horizontal Radiative Imbalance and Circulations

Picture is from IPCC 1995

Imbalanced horizontal distribution of radiative heating

(1) Latitudinal Imbalance between Pole and Tropics Timescale=1year

Driving Forces of Climate

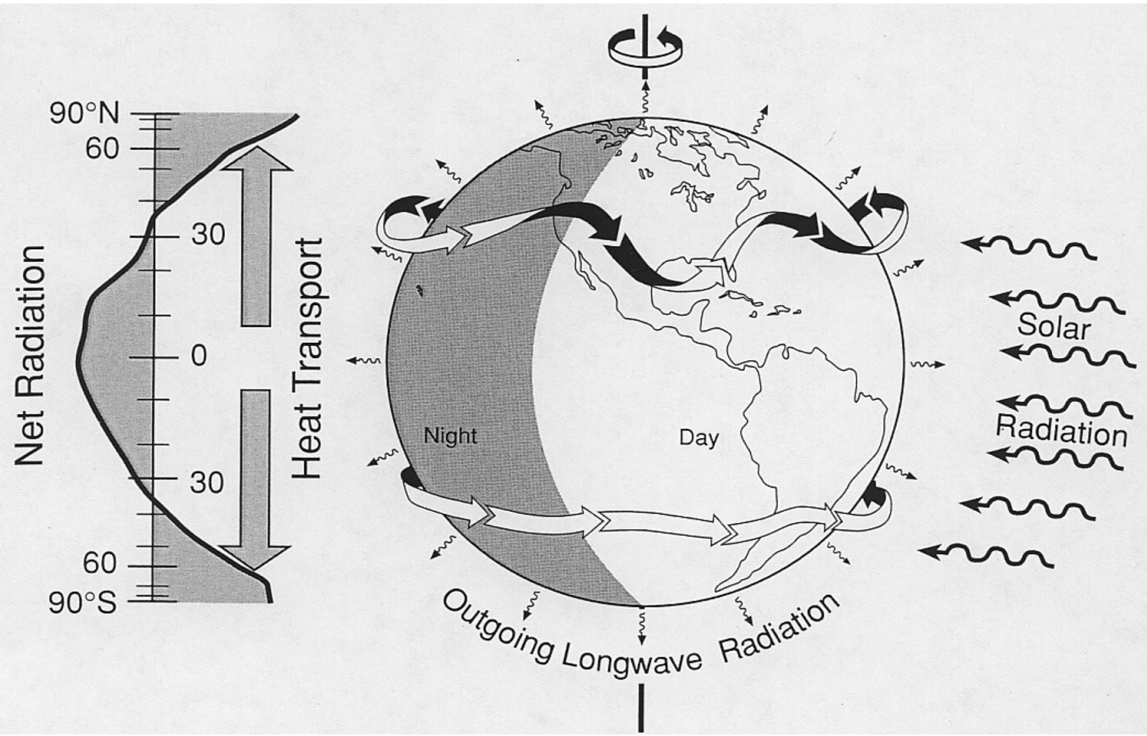

- Relaxation time to radiative equilibrium temperature (radiative equilibrium timescale) is estimated as about 30 days.
- Radiative imbalance between Pole and Tropics drives global circulations.
- Radiative imbalance between day and night has small influence on global circulations directly.

(2) Longitudinal Imbalance between Day and Night Timescale=1day

Diurnal Cycle of Precipitation from TRMM

From Takayabu, Y.N., 2002: GEOPHYSICAL RESEARCH LETTERS, VOL. 29, NO. 12, 1584, 10.1029/2001GL014113.

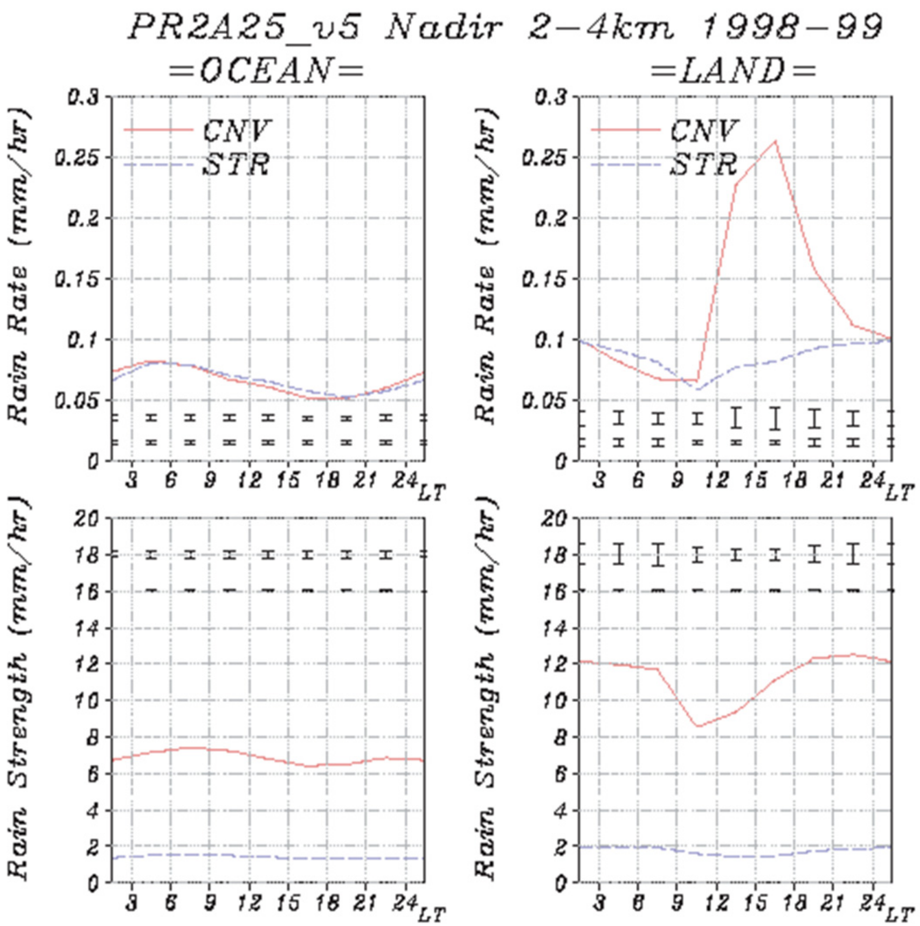

From Arakawa, O. and A. Kitoh at MRI/JMA

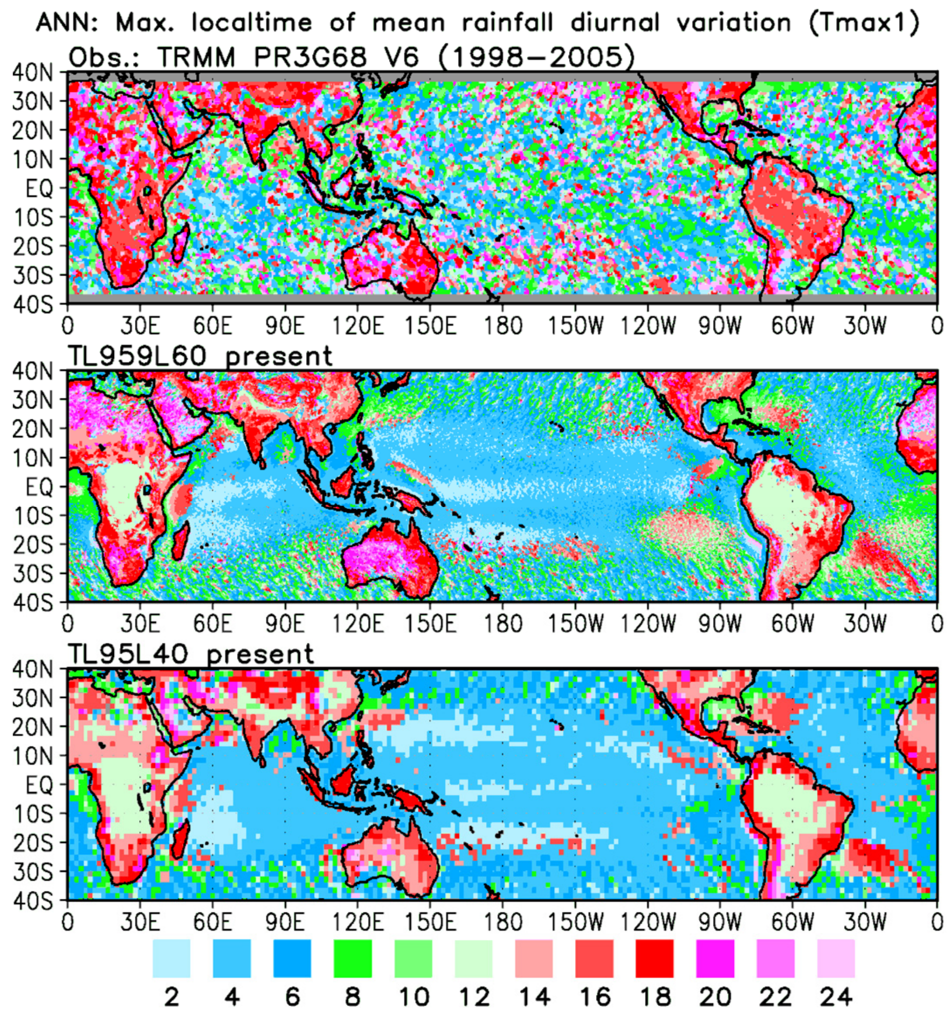

Diurnal Precipitation near Coastal Area

Diurnal Precipitation Regimes in the Global Tropics*

KAZUYOSHI KIKUCHI AND BIN WANG+

Department of Meteorology, and International Pacific Research Center, University of Hawaii at Manoa, Honolulu, Hawaii

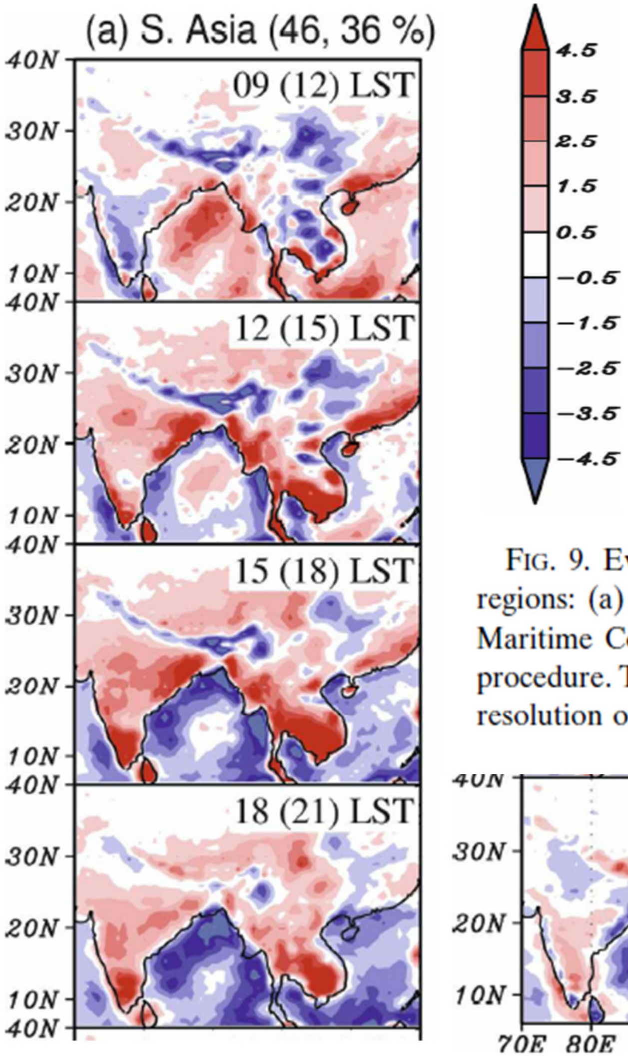

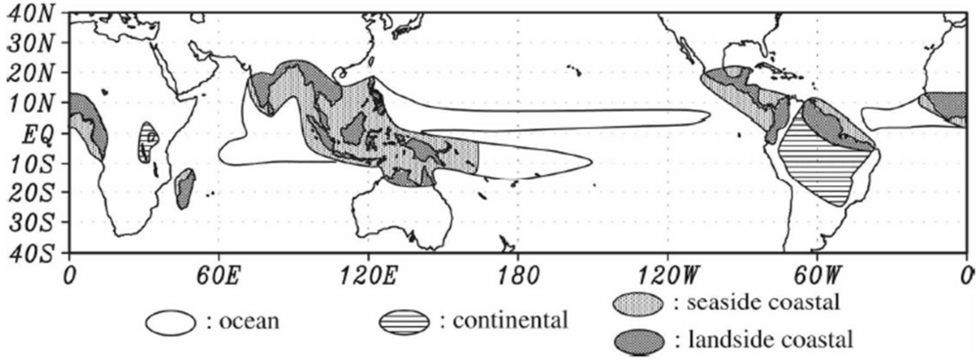

FIG. 10. Schematic diagram showing the global tropical diurnal precipitation regimes. Three regimes, namely oceanic, continental, and coastal regimes, are identified according to the amplitude, peak time, and phase propagation characteristics of the diurnal precipitation.

FIG. 9. Evolution of precipitation represented by the combination of $EEOF_1$ and $EEOF_2$ for the following regions: (a) South Asia, (b) Central America and northwest part of America, (c) West Africa, (d) Indonesia Maritime Continent, (e) South America, and (f) Madagascar. See the text for the complete description of the procedure. The corresponding modified LSTs are shown at the right corner of panels in (a) and (d). The horizontal resolution of the EEOFs is $0.75° \times 0.75°$.

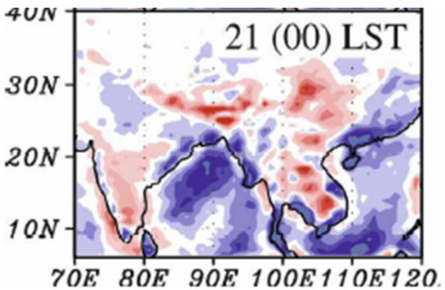

Meridional distribution of Annual mean radiation balance

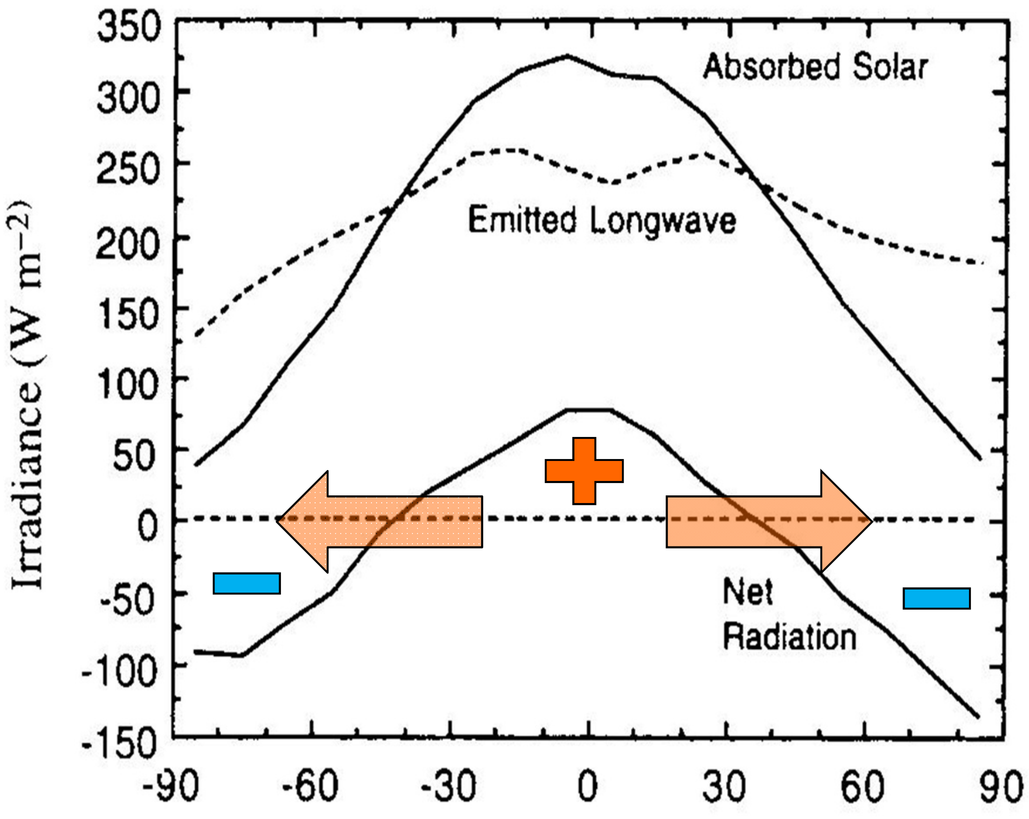

Hartmann (1994)

- **Solar radiation**
  - **Global mean : 235 Wm^{-2}**
  - **Low latitude : over 300 Wm^{-2}**
  - **Poles : about 50 Wm^{-2}**
- **Terrestrial radiation**
  - **Global mean : 235 Wm^{-2}**
  - **Less gradient between low latitudes and poles compared to that in solar radiation**
- **Net radiation**
  - **Global mean : 0 Wm^{-2}**
  - **Positive in low latitudes, negative in high latitudes**
- **Poleward heat transport by the atmosphere and ocean balances this meridional heat imbalance**

Observed annual mean SST, surface wind, precipitation

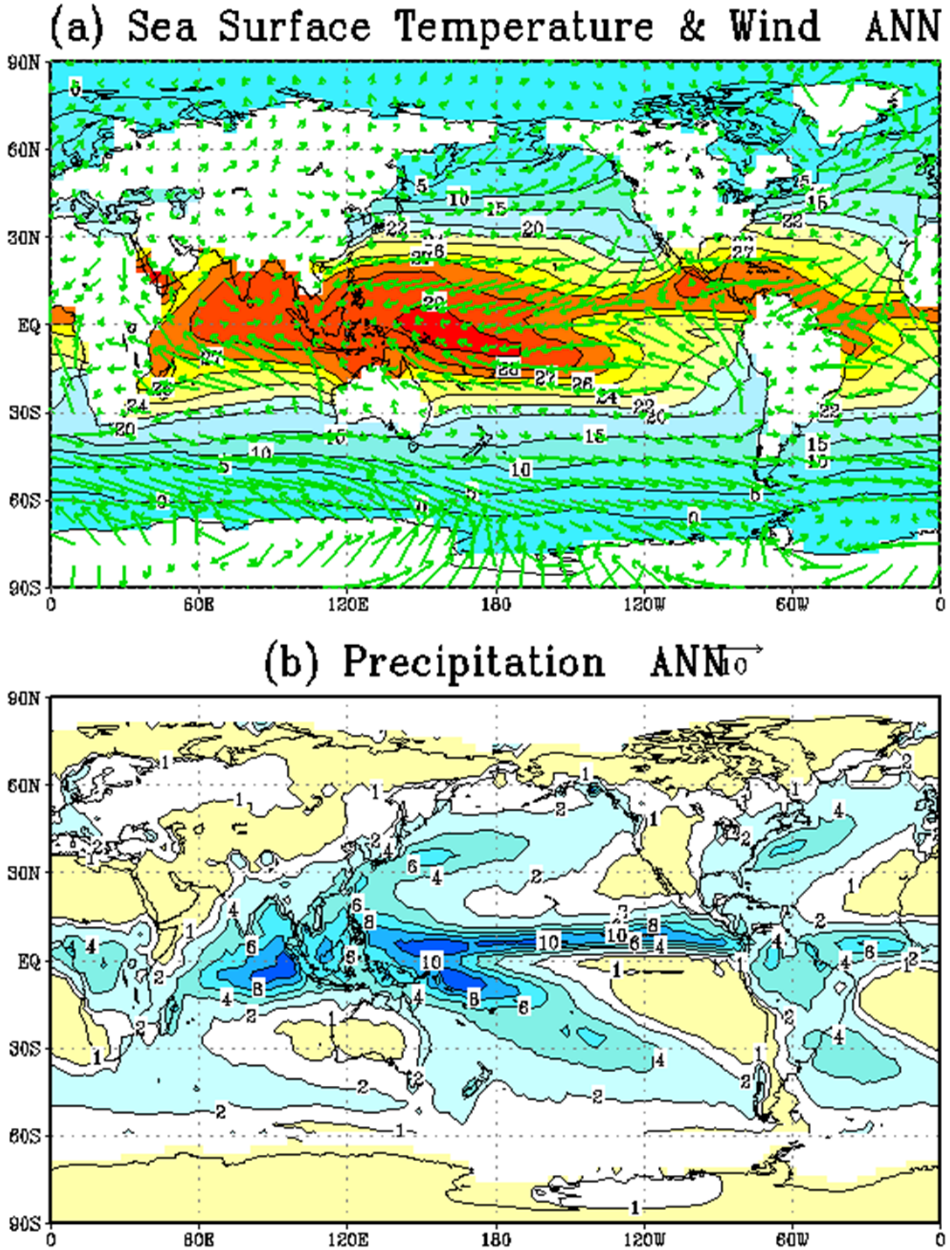

From Webster, P. J., 1994: The role of hydrological processes in ocean-atmosphere interactions, *Review of Geophysics*, **32**,427-476.

Sea surface temperature (SST) and Cumulus

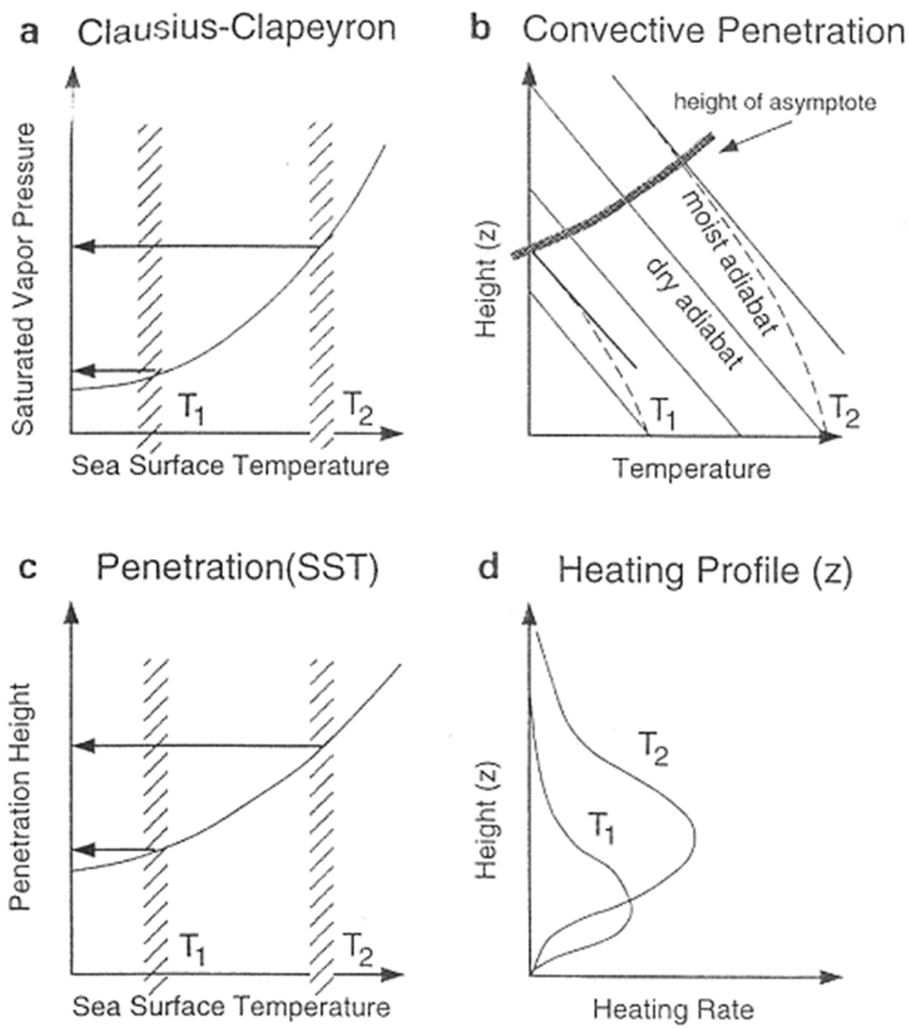

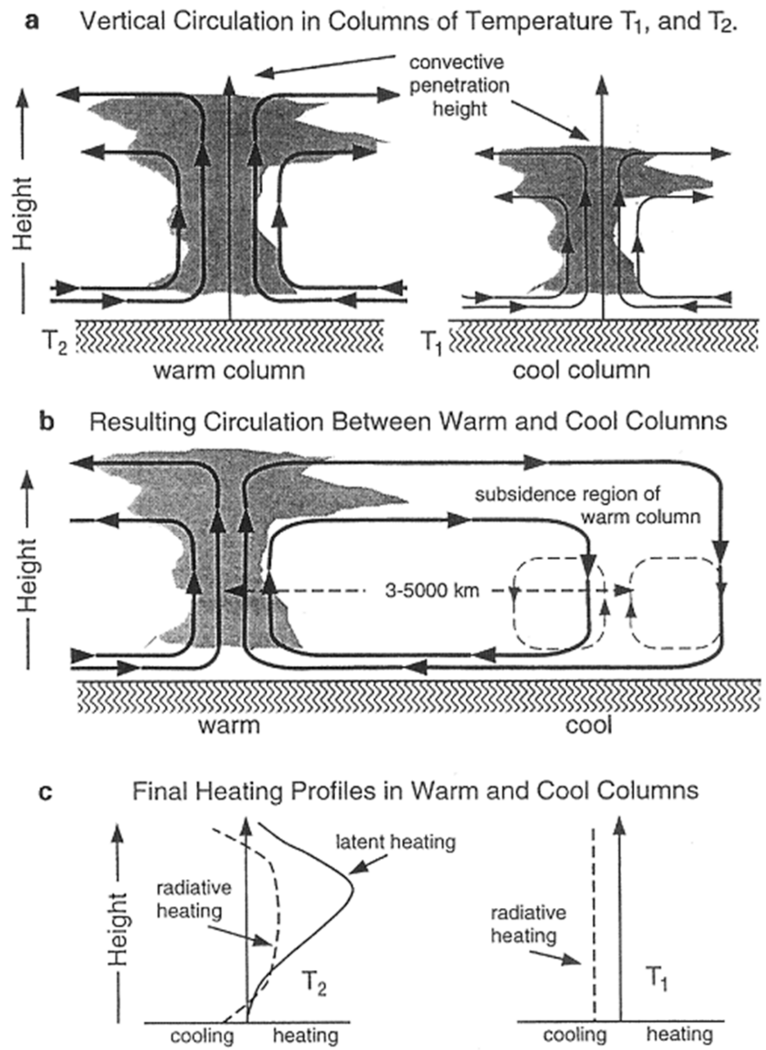

From Wallace, J.M. and P. V. Hobbs, 2006: Atmospheric Science. Academic Press, 483pp.

Energy Transport by Atmospheric Circulation

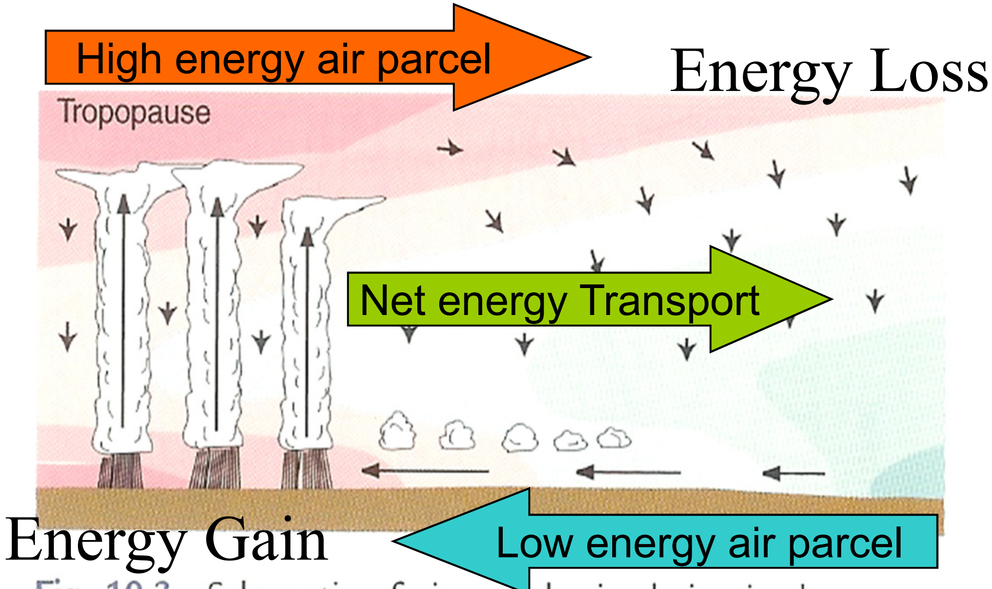

Fig. 10.3 Schematic of air parcels circulating in the atmosphere. The Colored shading represents potential temperature or moist static energy, with pink indicating higher values and blue lower values. Air parcels acquire latent and sensible heat during the time that they reside within the boundary layer, raising their moist static energy. They conserve moist static energy as they ascend rapidly in updrafts in clouds, and they cool by radiative transfer as they descend much more slowly in clear air.

- Moist Static Energy

  $H=CpT+gZ+Lq$

  T: Temperature
  Z: Height
  q: Specific Humidity

H of air parcels is conserved even through adiabatic process and/or condensation process,

but, not conserved through the processes of radiation, heat and moisture supply from ground surface.

Heat transport by the atmosphere and ocean

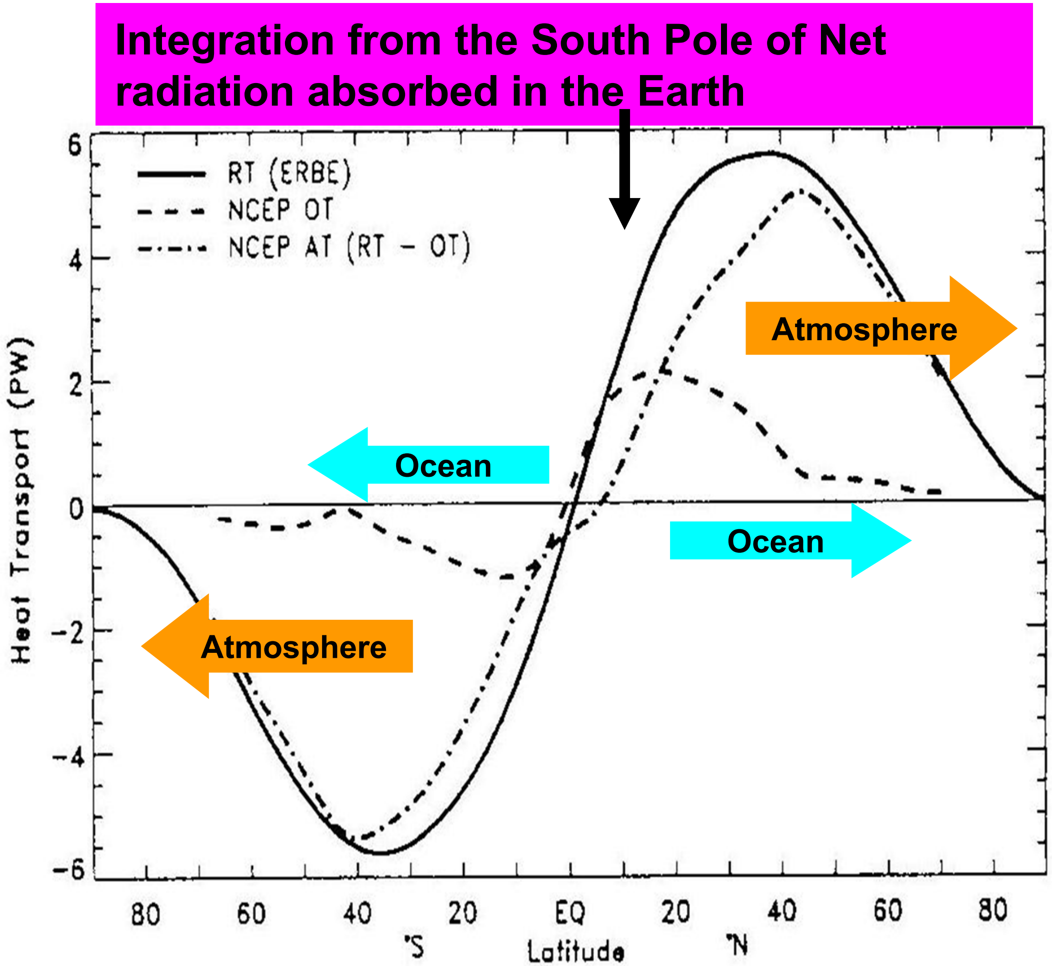

Trenberth and Caron (2001)

- Implied heat transport from top of atmosphere (TOA) radiation balance
  - Integrate net radiation from pole to pole
- Both the atmosphere and ocean are responsible for heat transport
- Atmospheric transport is larger, particularly in the mid and high latitudes
- Oceanic heat transport is large in low-latitudes

Atmospheric global circulations driven by latitudinal heating contrast

From Wallace, J.M. and P. V. Hobbs, 2006: Atmospheric Science. Academic Press, 483pp.

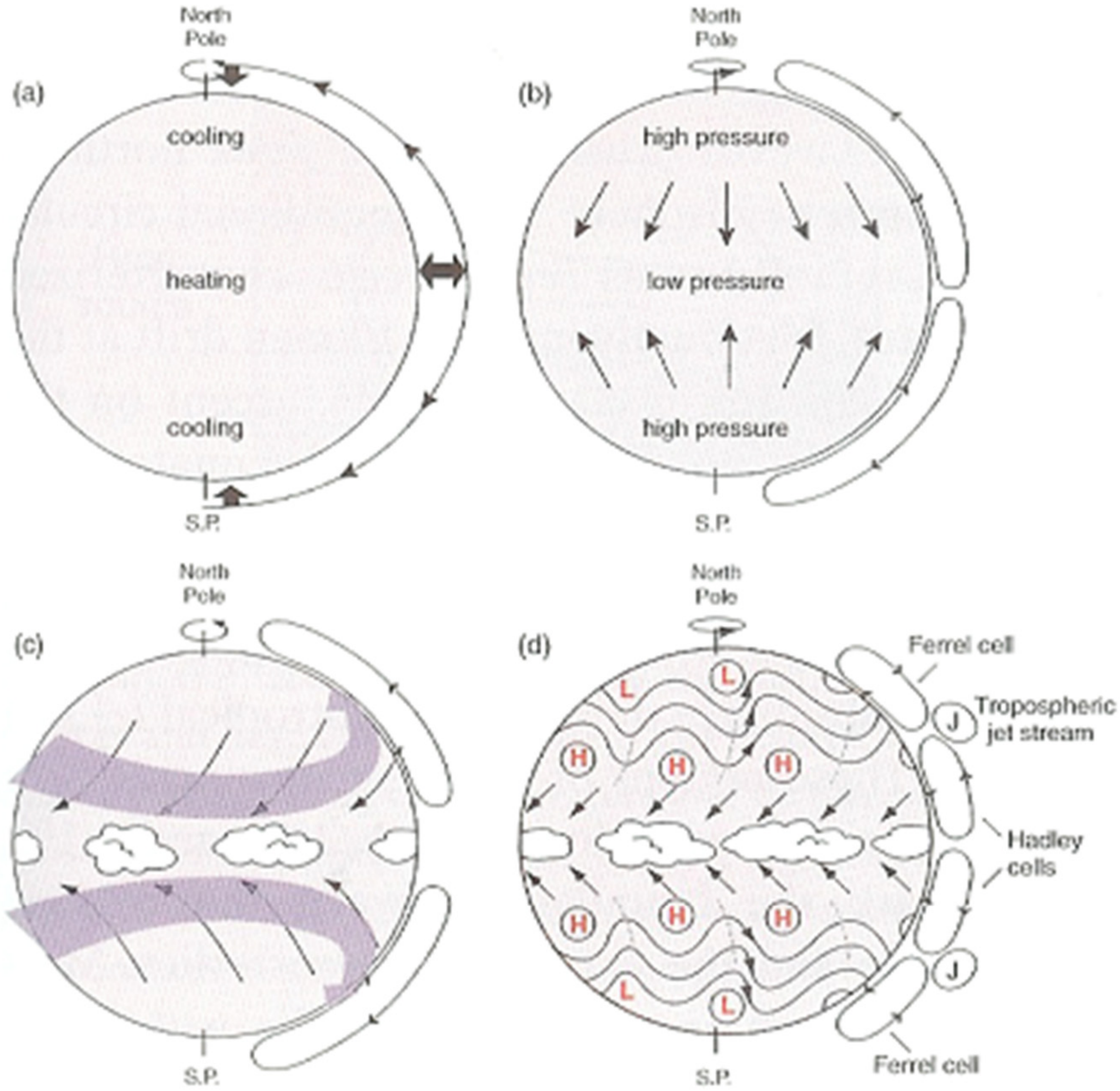

Fig. 7.21 Schematic depiction of the general circulation as it develops from a state of rest in a climate model for equinox conditions in the absence of land–sea contrasts. See text for further explanation.

Ose,T., 1989: Hadley circulations and penetrative cumulus convection. J.Meteor.Soc.Japan, **67**, 605-619.

Hadley (direct) circulation

These are model results.

(1) There are two direct and one indirect circulations.

100hPa

1000hPa

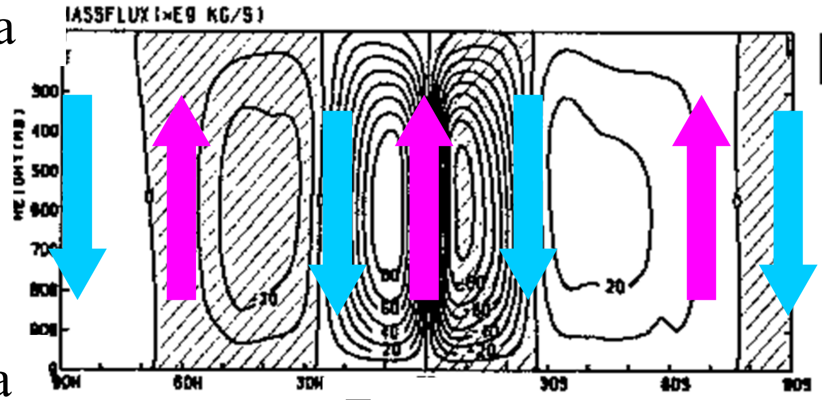

Equator

Stream-function

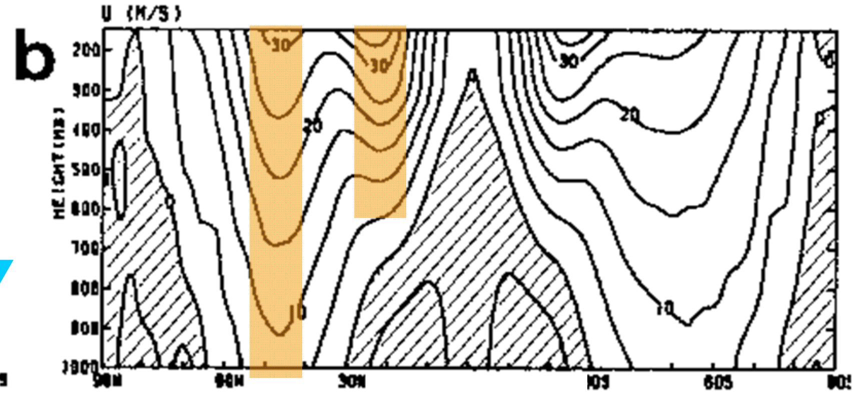

Equator

Zonal wind

(2) After zonal waves are removed in the model, Hadley circulations and subtropical jets are left.

100hPa

1000hPa

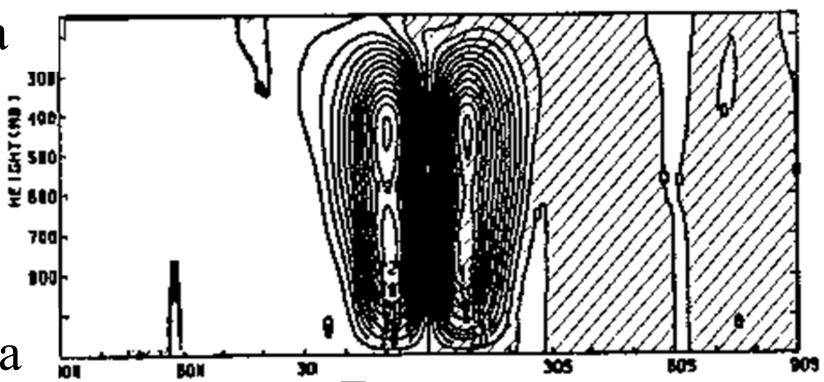

Equator

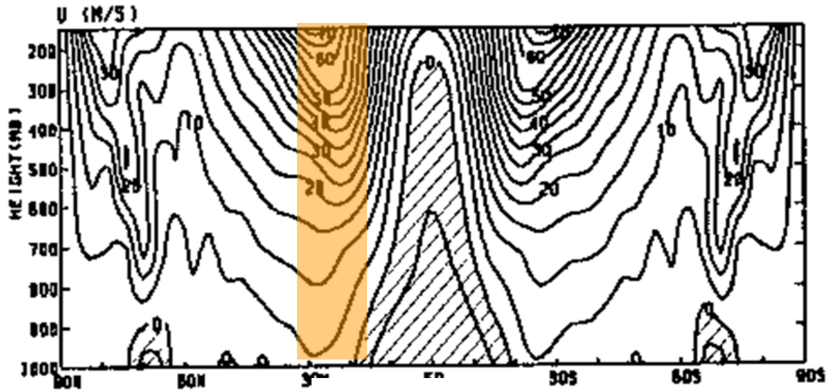

Equator

From James, I. N., 1995: Introduction to Circulating Atmospheres. Cambridge University Press, 422pp.

Ferrel (in-direct) circulation.

Three mechanisms to drive meridional mass circulations

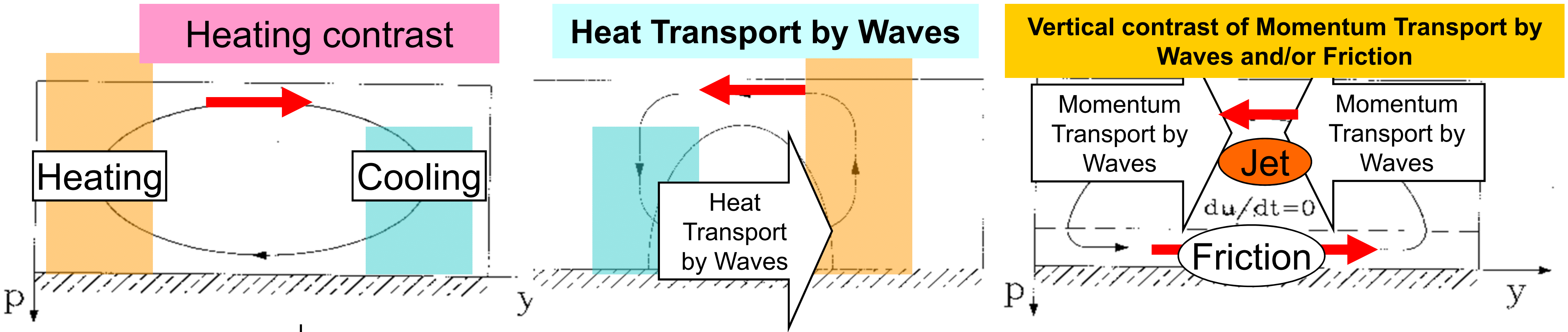

Primary mechanism for Hadley Circulation

Primary mechanism for Ferrel Circulation

Mean meridional Circulations depend on vertical coordinates.

Iwasaki, T., 1989: A diagnostic formulation for wave–mean flow interactions and Lagrangian-mean circulation with a hybrid vertical coordinate of pressure and isentropes. *J. Meteor. Soc. Japan,* **67,** 293–312.

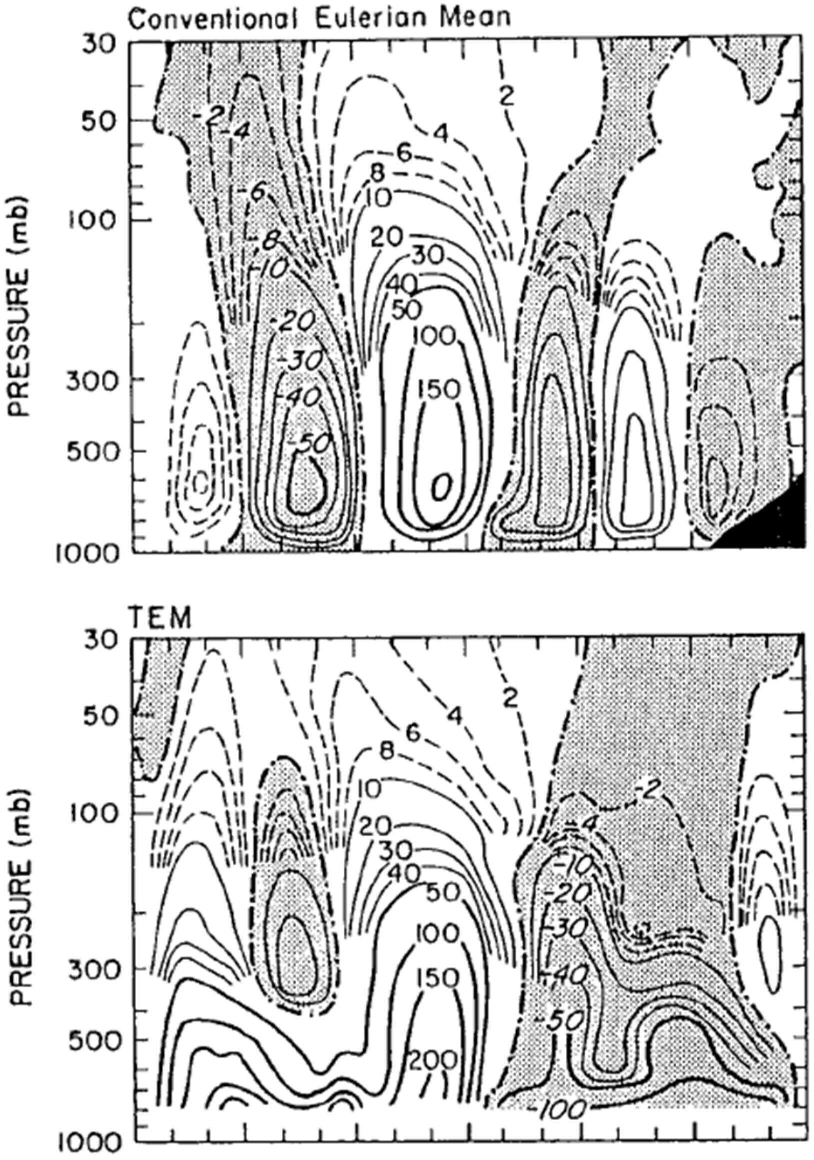

Lagrangian Mean

Net mass transport including wave effect

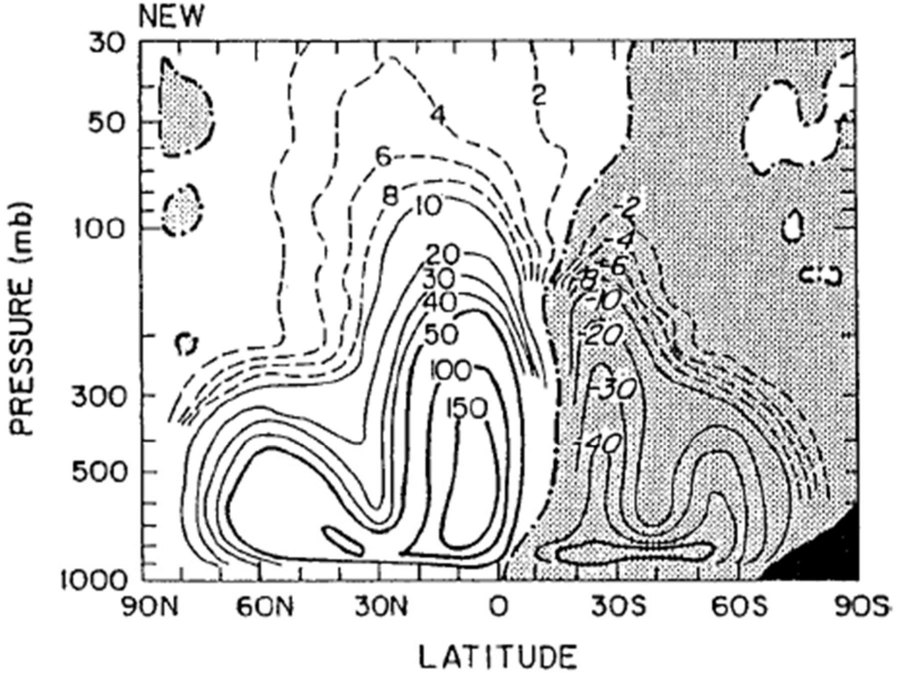

FIG. 1. Mass streamfunctions of the perpetual Jan simulation by the National Center for Atmospheric Research Community Climate Model version 1, diagnosed with the conventional Eulerian mean, the TEM, and the p_φ analyses. Contour values are shown with units of $\times\ 10^9\ \mathrm{kg\ s^{-1}}$ (after I89).

Seasonal Change

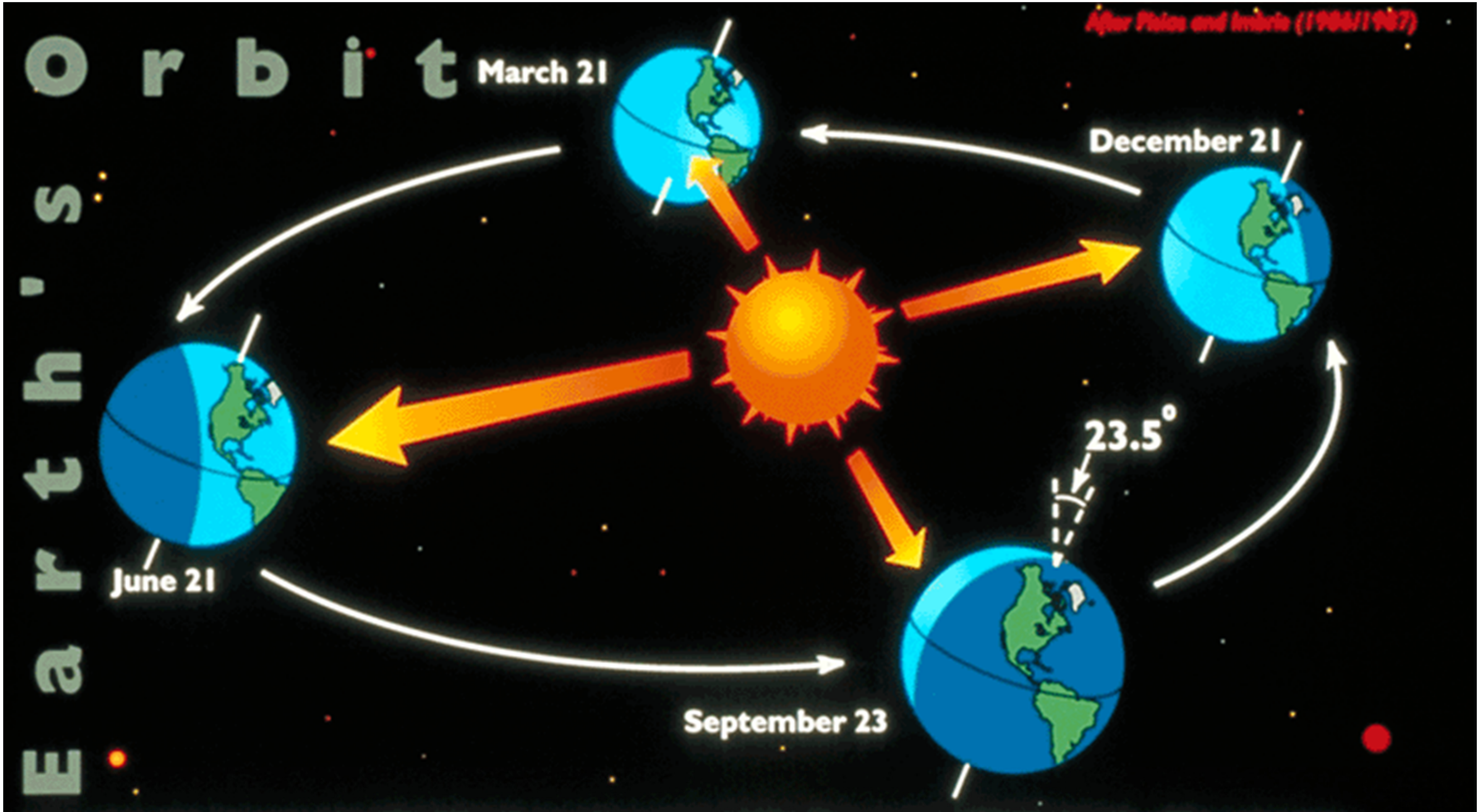

Viewed in the present, the tilted Earth revolves around the Sun on an elliptical path. The orientation of the axis remains fixed in space, producing changes in the distribution of solar radiation over the course of the year. These changes in the pattern of radiation reaching Earth's surface cause the succession of the seasons. The Earth's orbital geometry, however, is not fixed over time. Indeed, long-term variations in the Earth's orbit help explain the waxing and waning of global climate in the last several million years.

Seasonal Change of Sea Surface Temperature (SST)

Solar Insolation

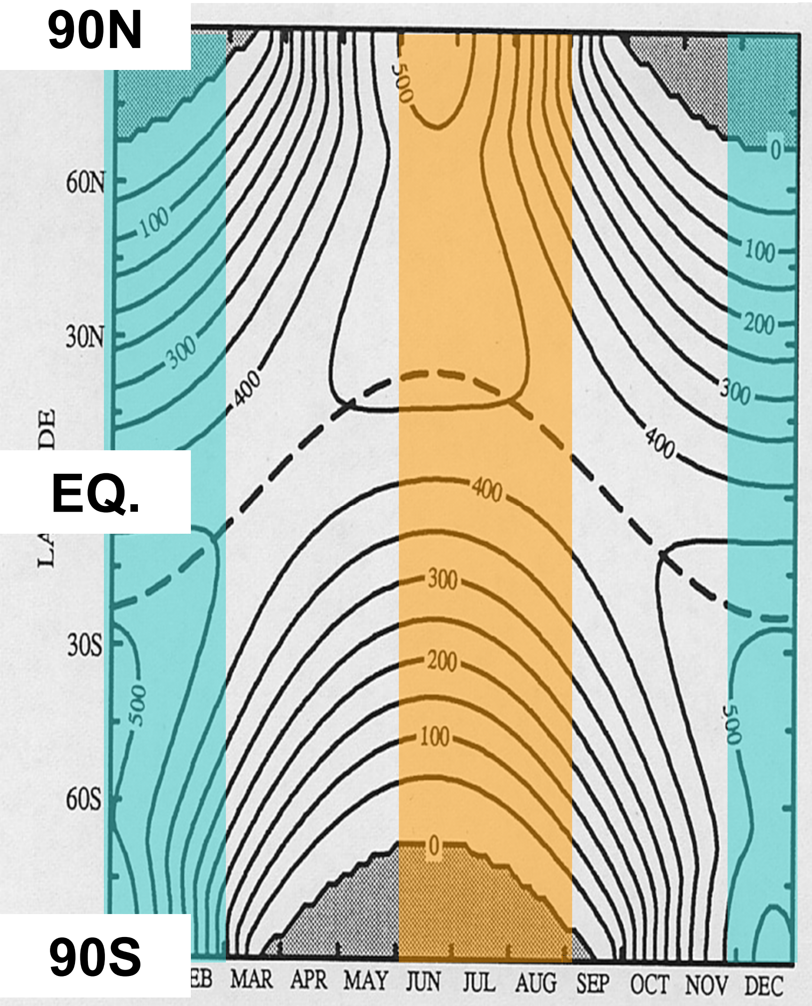

Dec.-Jan.-Feb.

Jun-July-August

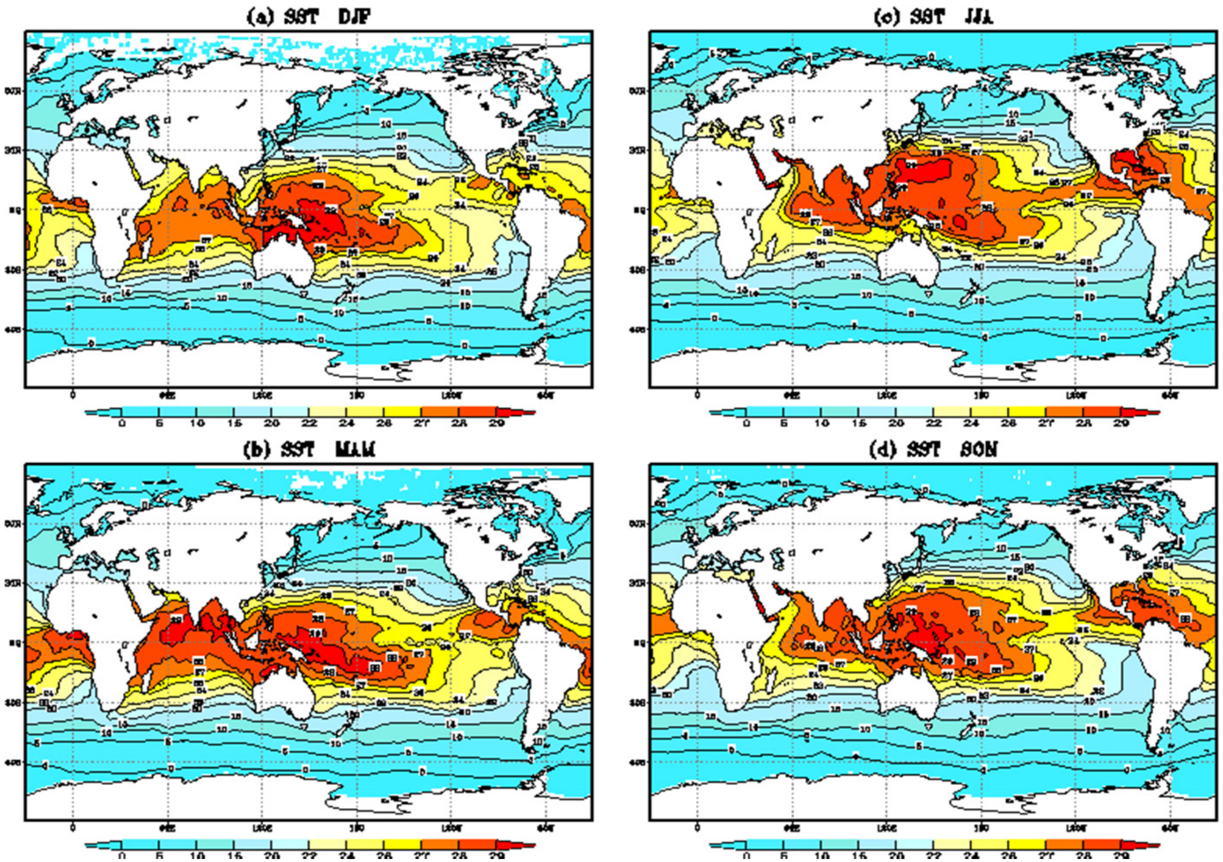

Mar.-Apr.-May

Sep.-Oct.-Nov.

SST and Precipitation in each season

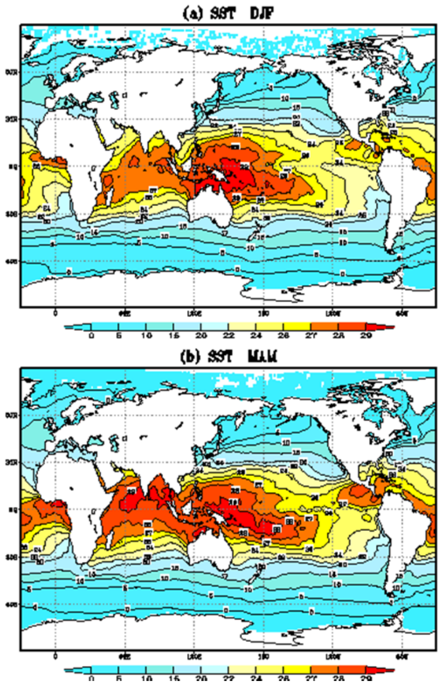

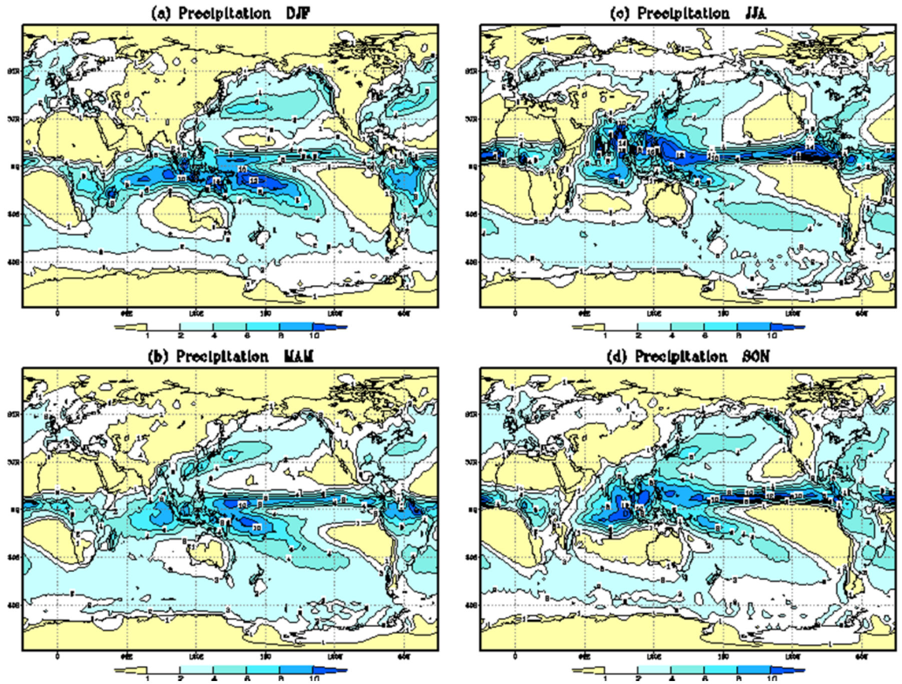

Seasonal Change of Temperature and Zonal Wind

Solar Insolation

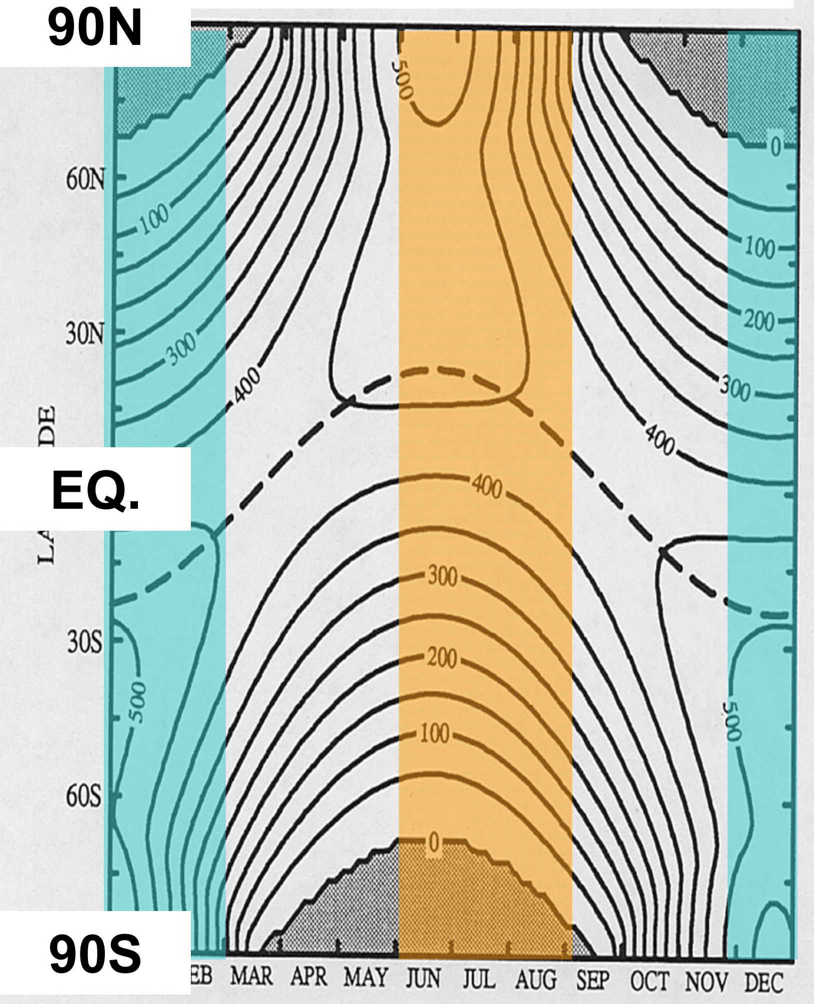

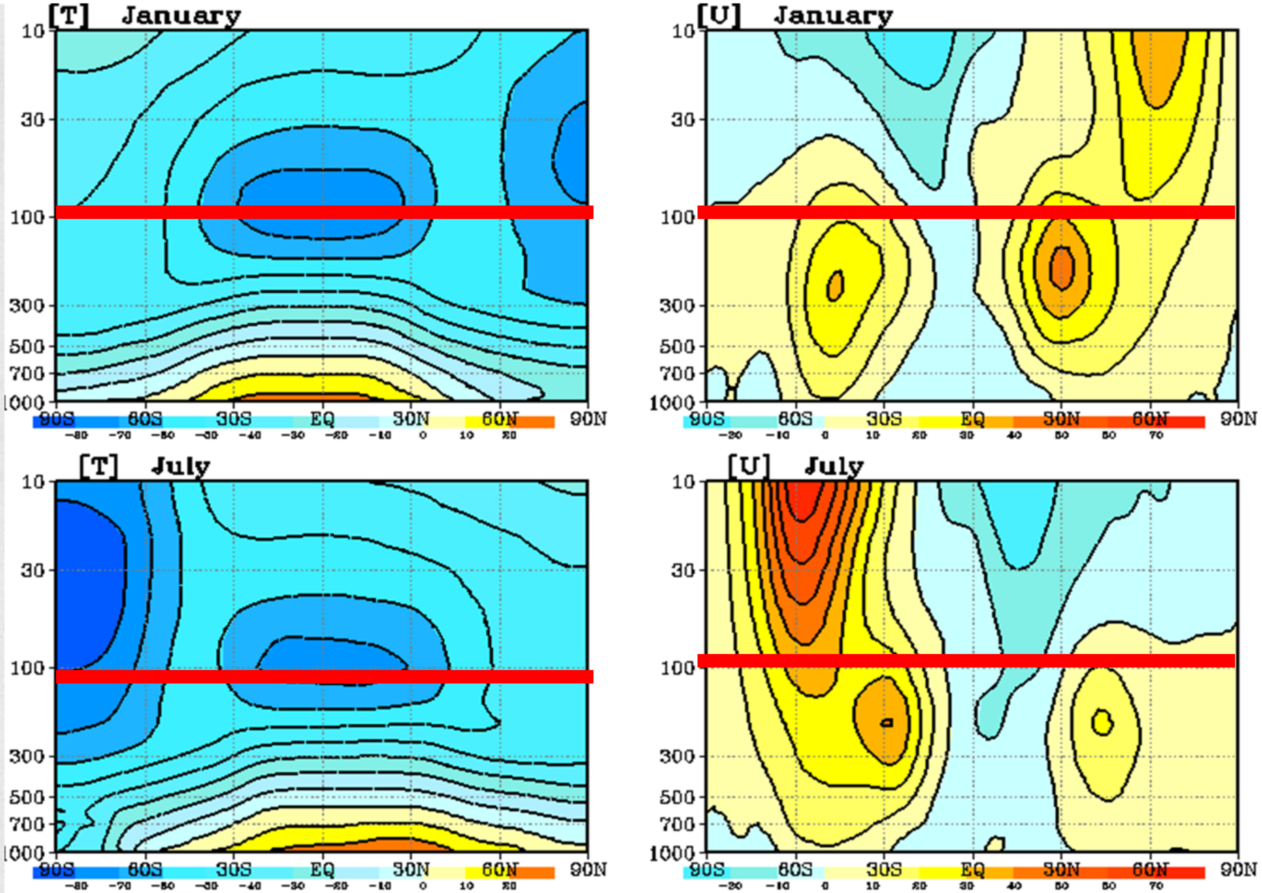

200 hPa and 850 hPa winds in JJA and DJF

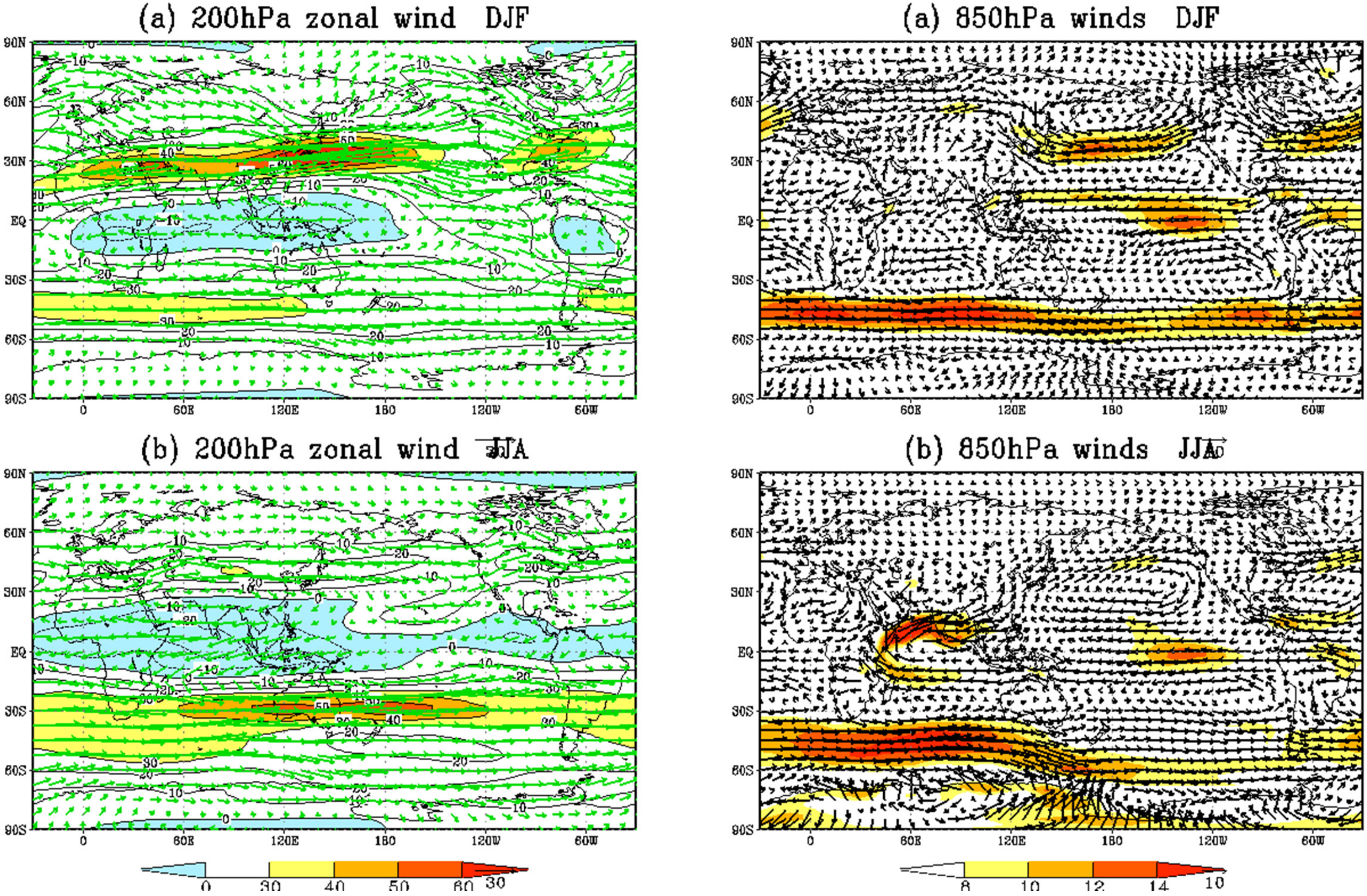

Jan-Jul contrast of surface temperature/precipitation

January Surface Air Temperature NCEP(1949–2000)

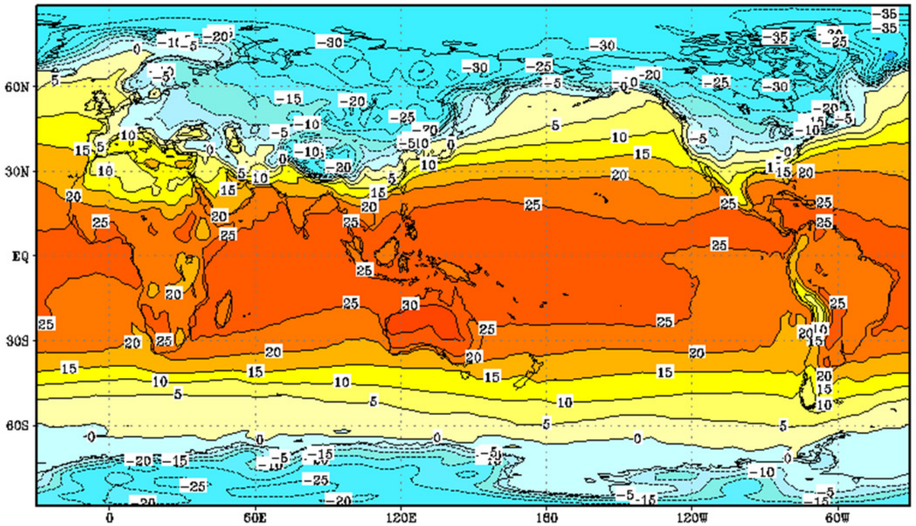

January Precipitation CMAP(1979–2001)

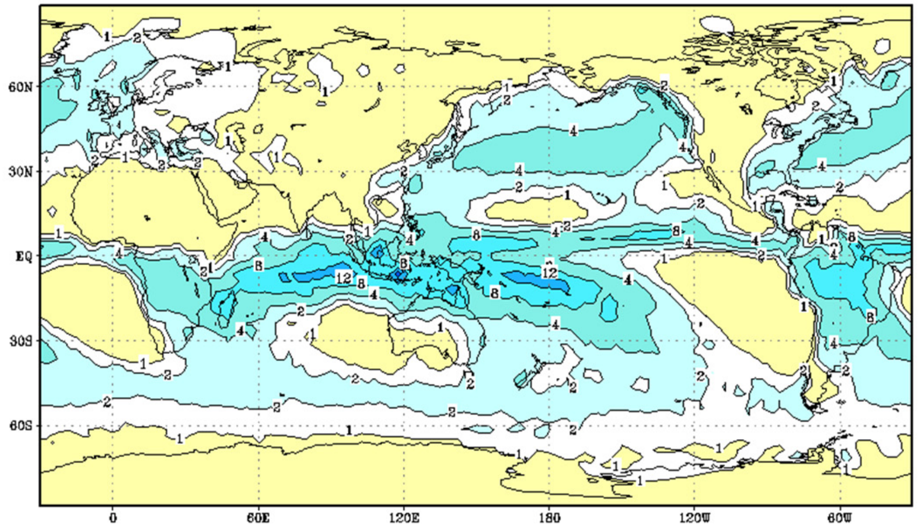

July Surface Air Temperature NCEP(1949–2000)

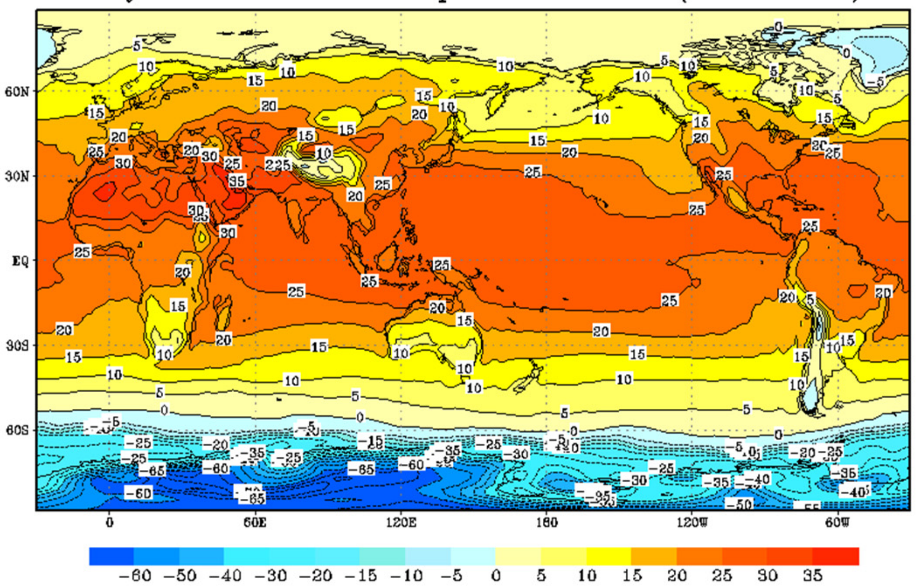

July Precipitation CMAP(1979–2001)

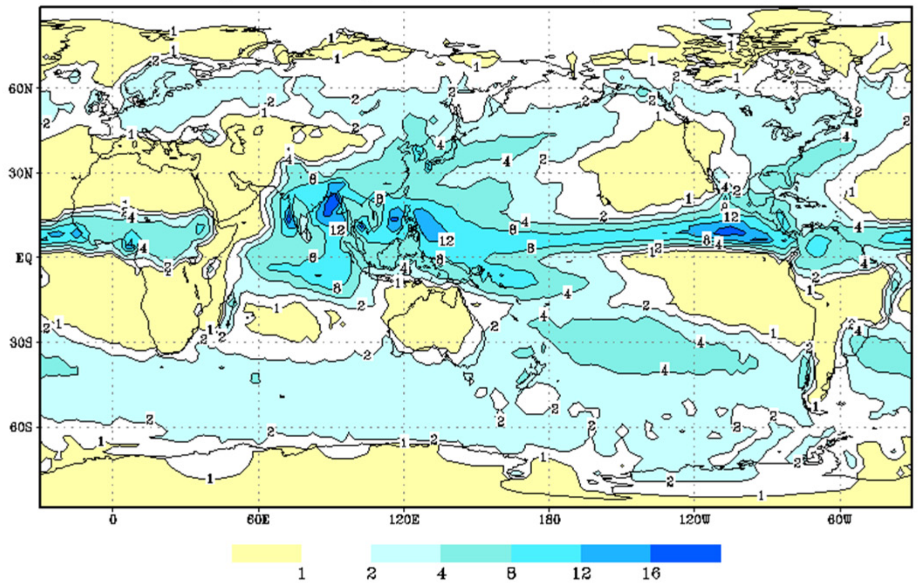

Northern Summer Monsoon

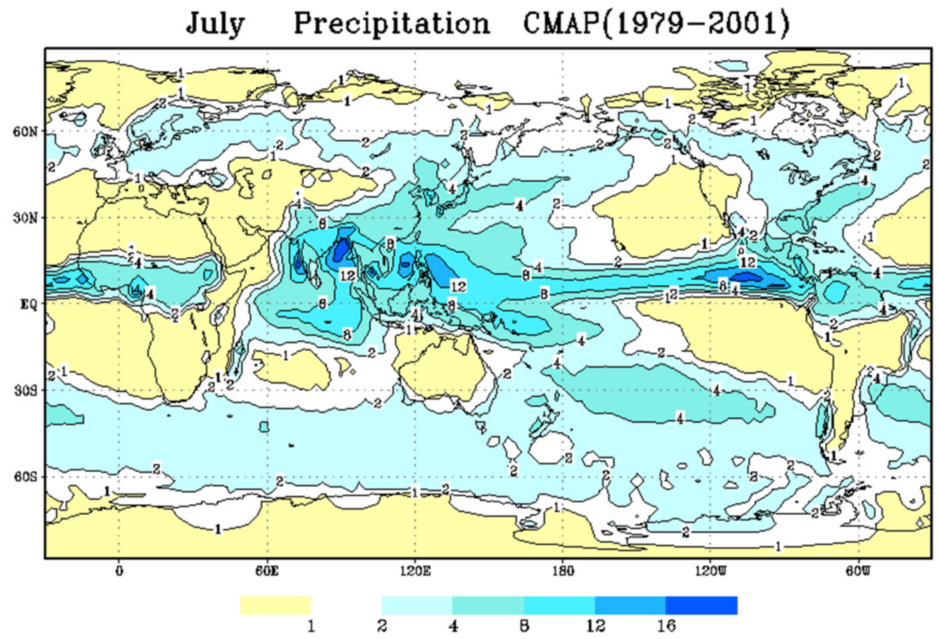

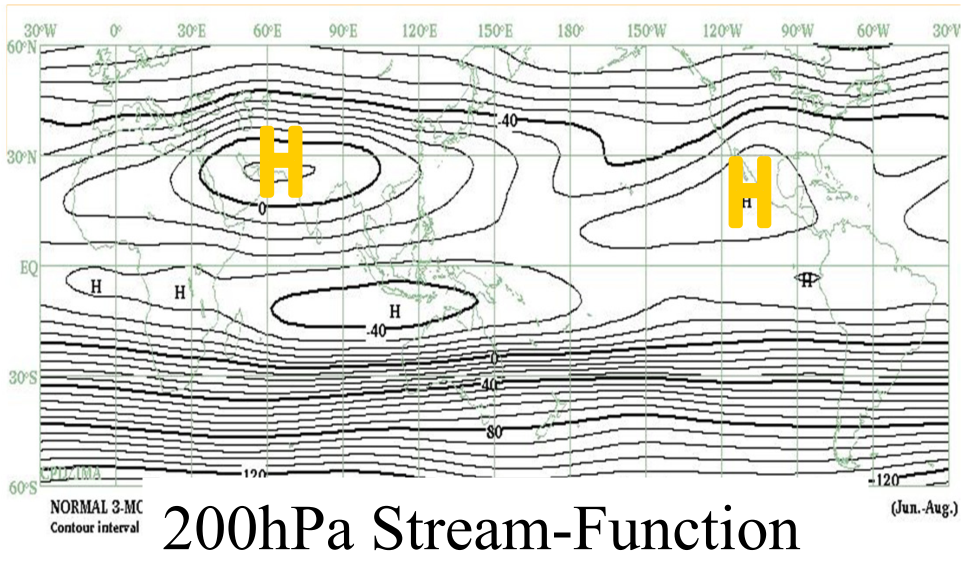

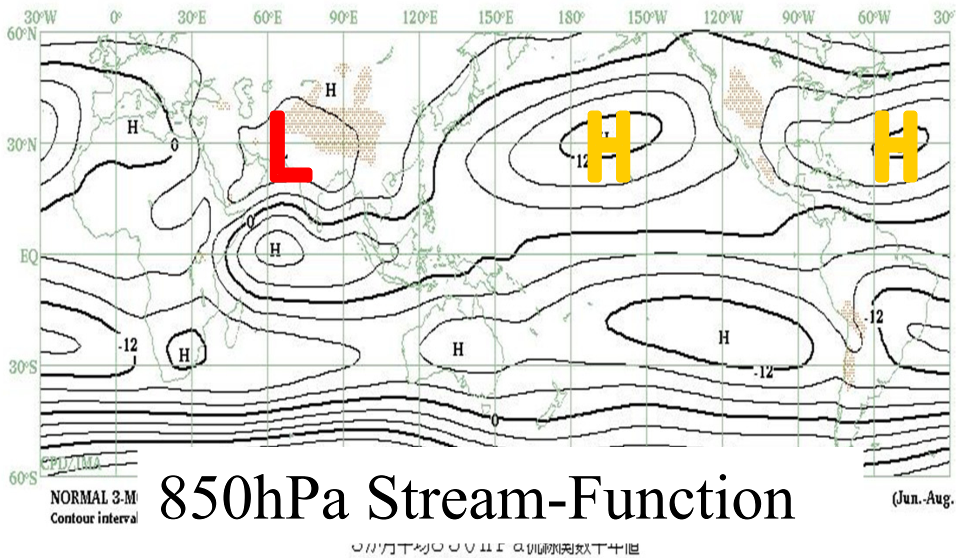

***Q. J. R. Meteorol.* SOC. (1996), 122**, pp. **1385-1404** Monsoons and the dynamics of deserts. By MARK J. RODWELL' and BRIAN **I.** HOSKINS

25N

Precipitation

10N

Precipitation

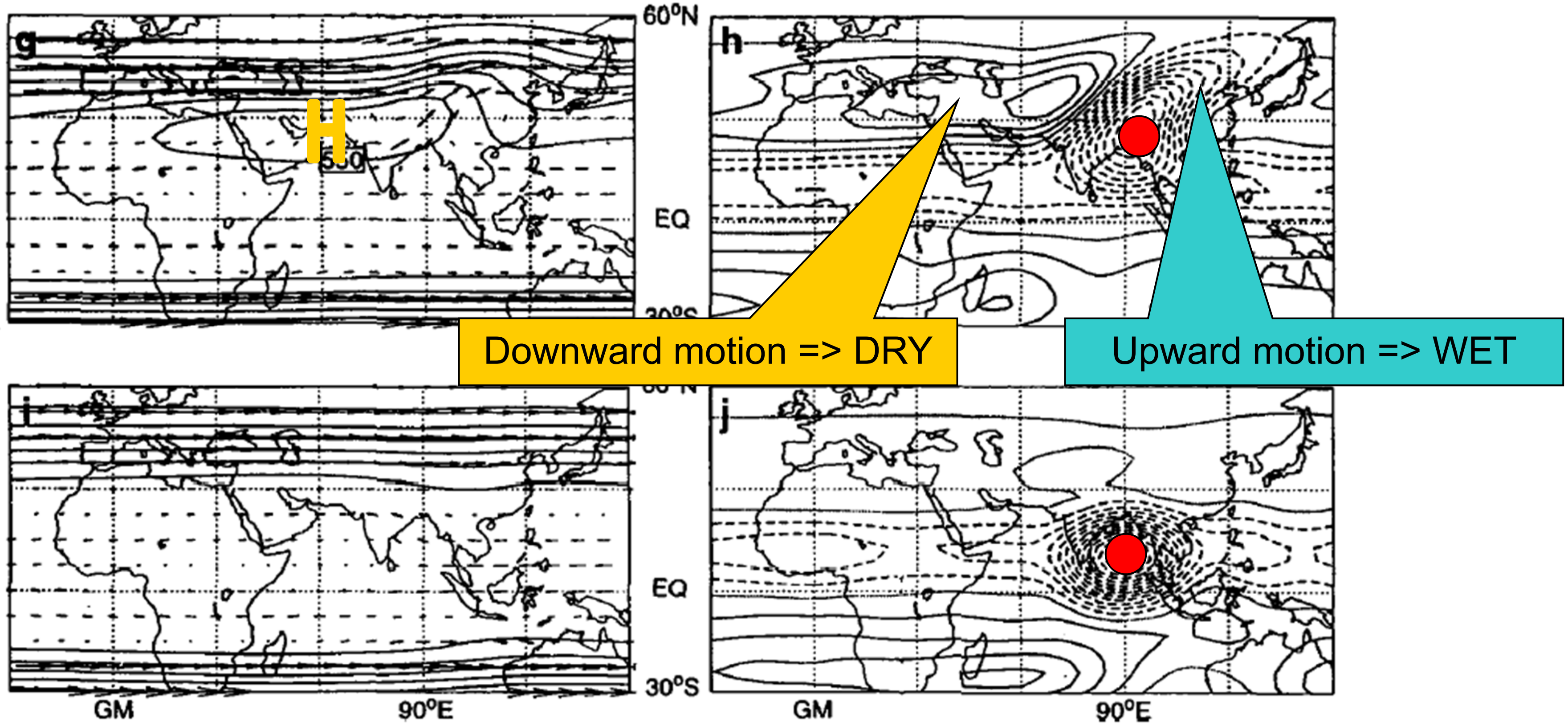

Figure 8. Day 11 of a series of integrations without orography. (a), (c), (e), (g) and (i) pressure and horizontal winds on the 325 K isentropic surface, with contour interval 40 hPa; (b), (d), (f), (h) and (j) vertical velocity at 477 hPa, with contour interval 0.25 hPa hr^{-1}; (a) and (b) integration linearized about a resting basic-state and forced with heating at 90°E, 25°N; (c) and (d) integration linearized about a resting basic-state and forced with heating at 25°N superimposed on the June to August zonal-mean flow; (e) and (f) integration linearized about the zonal-mean basic-state and forced with heating at 25°N; (g) and (h) non-linear integration forced with heating at 25°N; (i) and (j) nonlinear integration forced with heating at 90°E, 10°N.

Precipitation and Mountain

NOTES AND CORRESPONDENCE

Role of Narrow Mountains in Large-Scale Organization of Asian Monsoon Convection*

Shang-Ping Xie,+ Haiming Xu,# N. H. Saji, and Yuqing Wang+
International Pacific Research Center, SOEST, University of Hawaii at Manoa, Honolulu, Hawaii

W. Timothy Liu
Jet Propulsion Laboratory, Pasadena, California

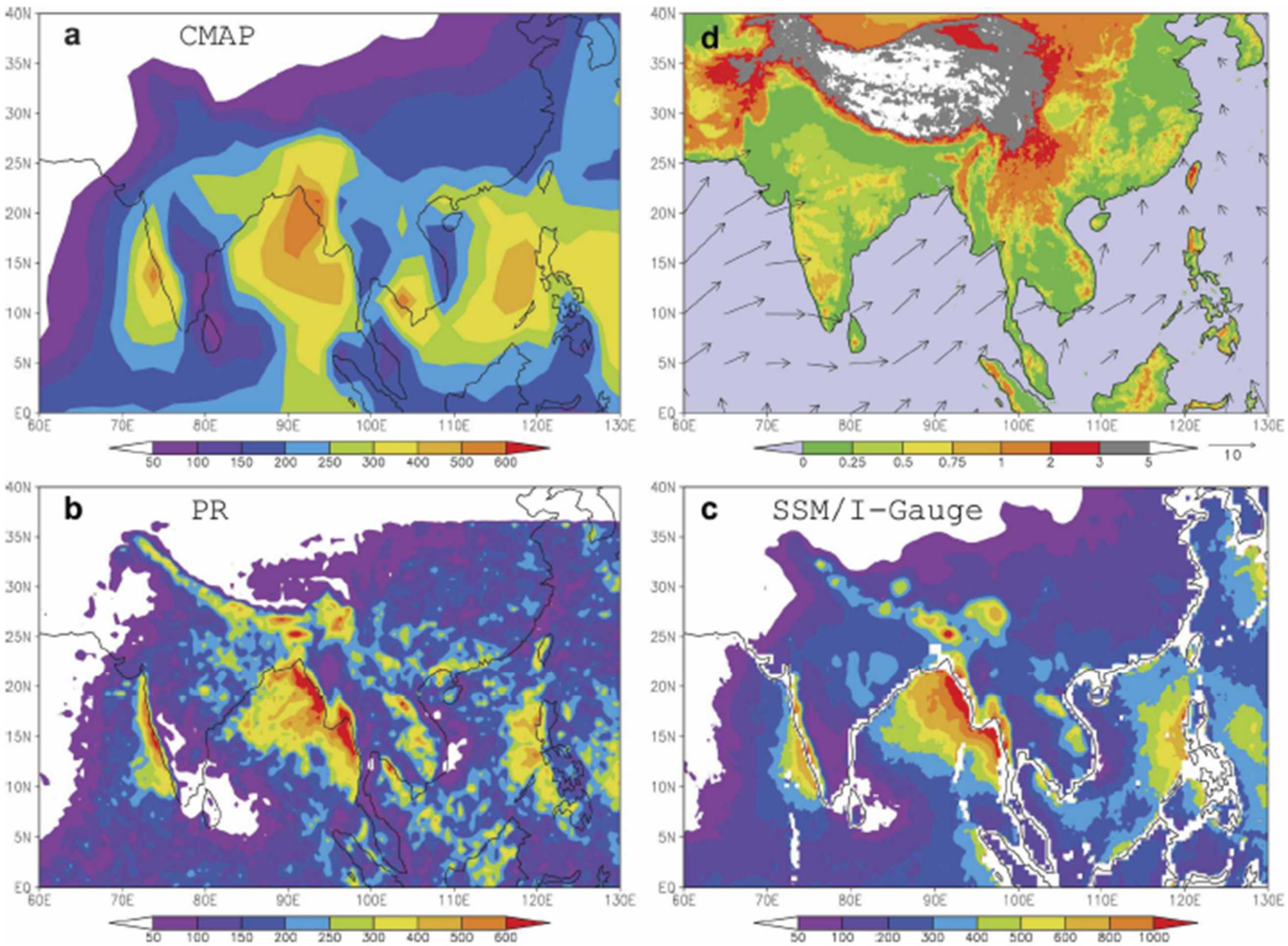

FIG. 1. Jun–Aug climatologies of surface precipitation (mm month^{-1}) based on (a) CMAP, (b) TRMM PR, and (c) SSM/I-gauge merged products. (d) Land orography (km) and QuikSCAT surface wind velocity (m s^{-1}).

Southern Summer Monsoon

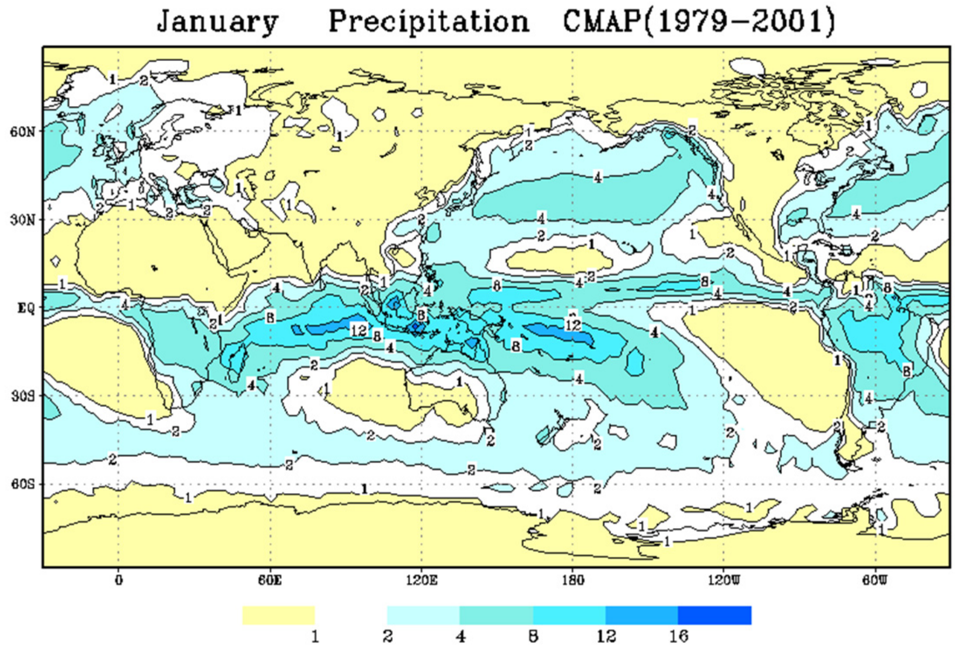

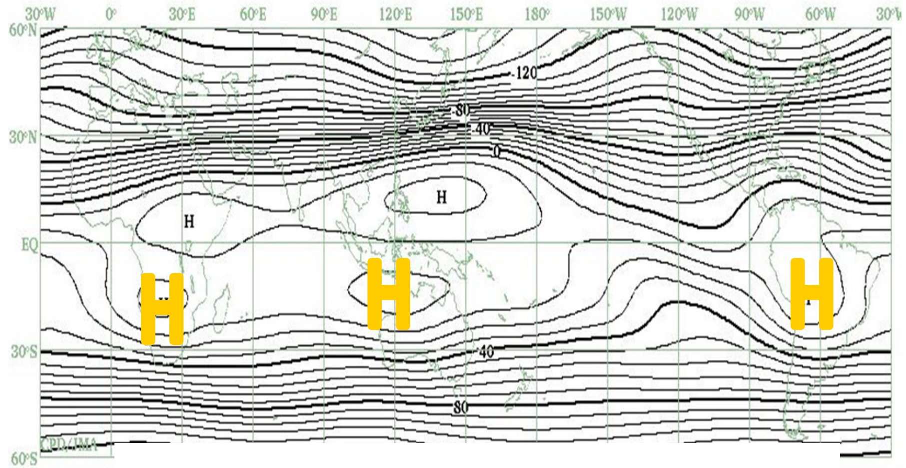

200hPa Stream-Function

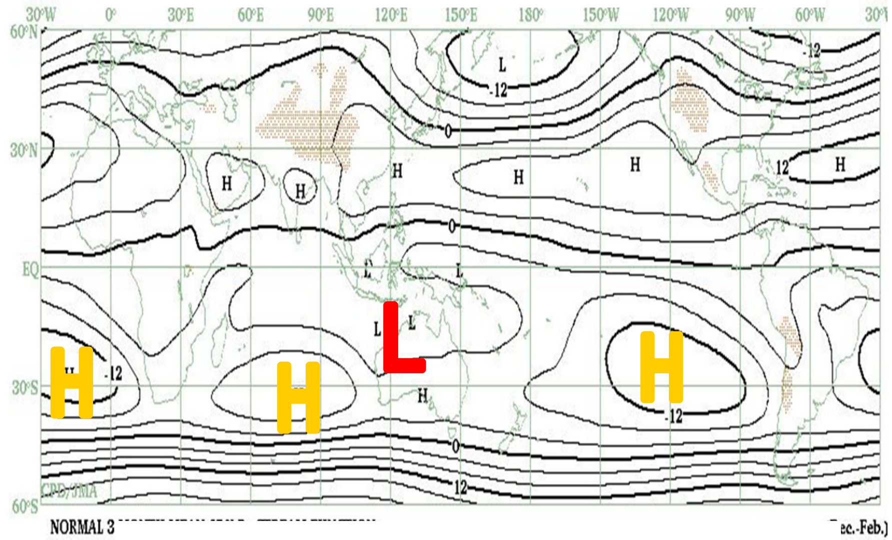

850hPa Stream-Function

Annual temperature range

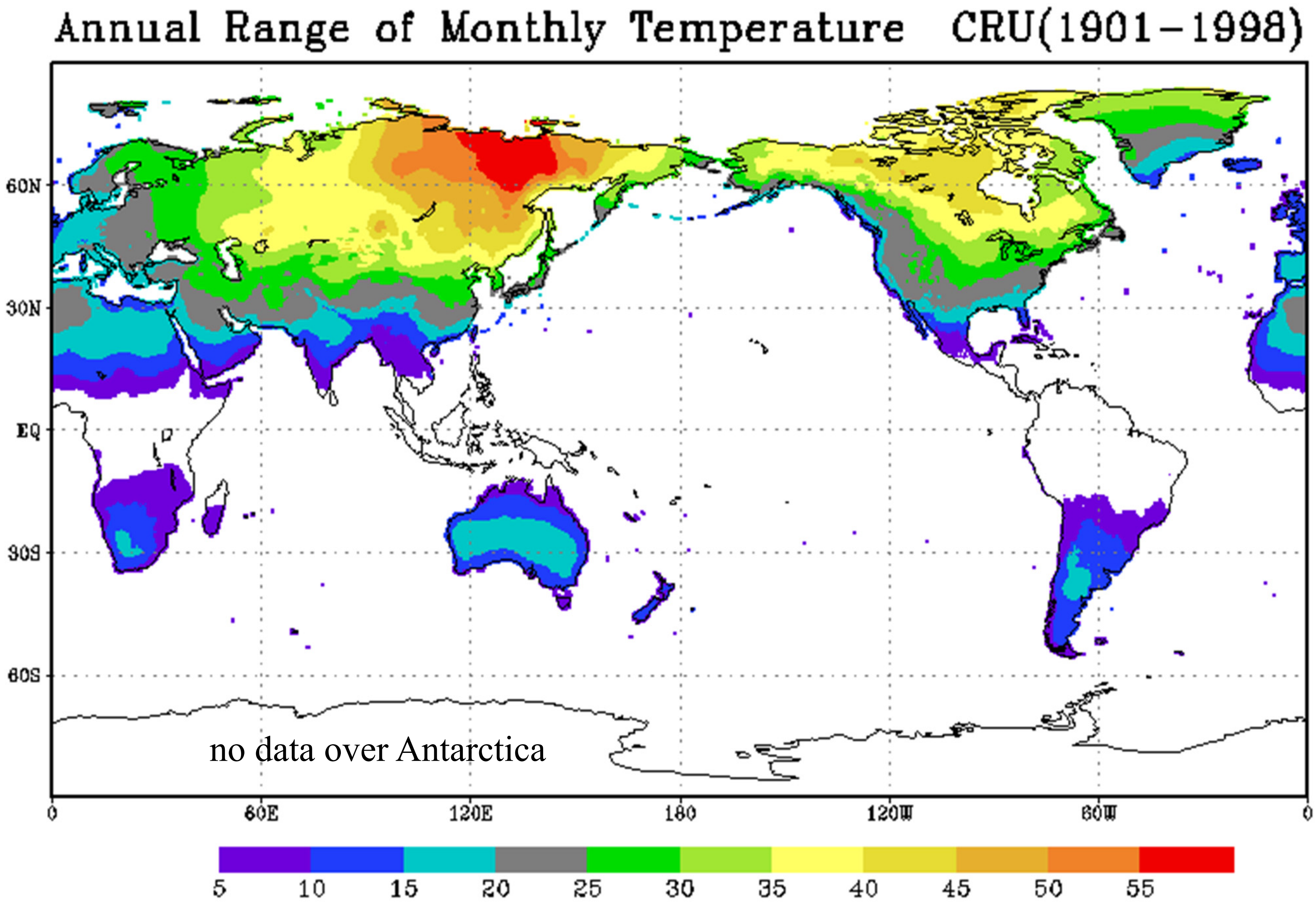

Month of maximum monthly mean temperature

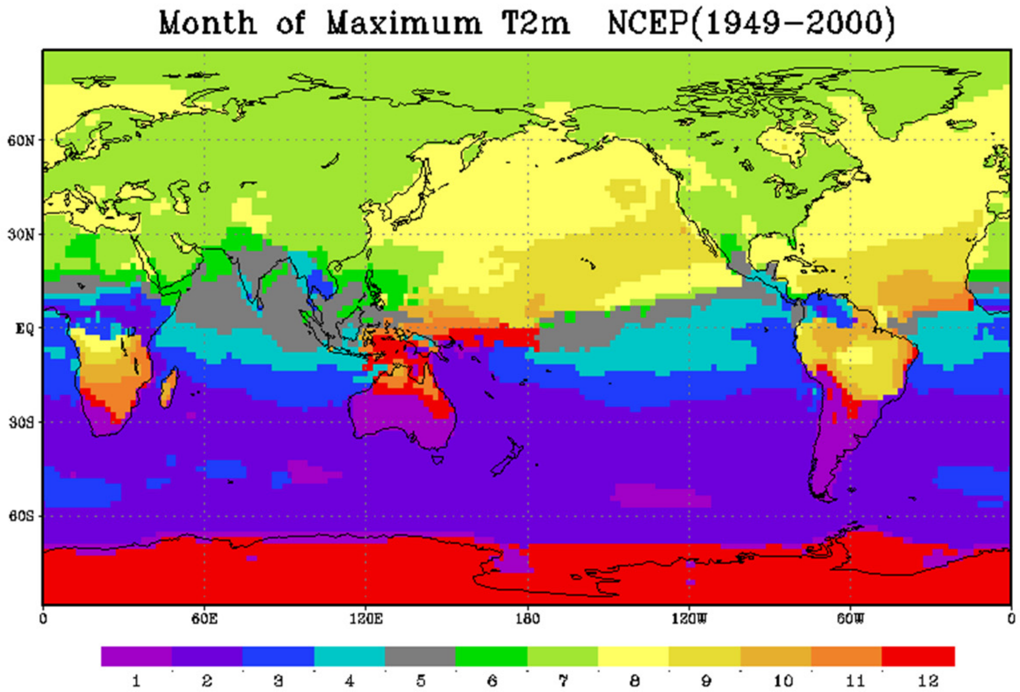

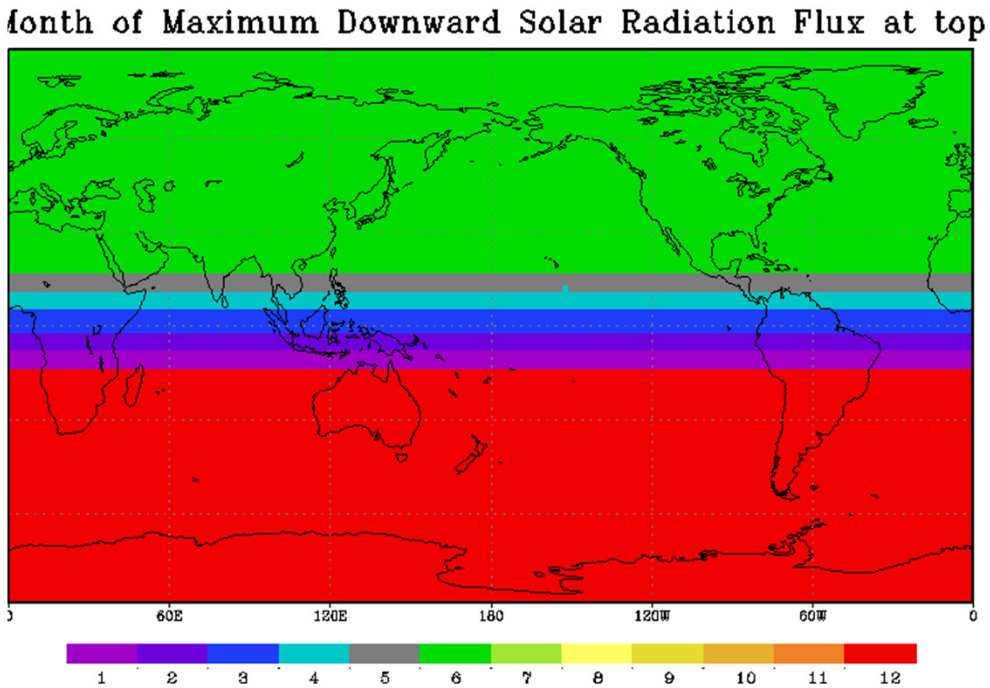

(Right) Downward solar radiation at the top of the atmosphere is maximum in June (December) poleward of about 15° latitude in the NH (SH). In the tropics, it is January, February, March, April and May at 10° S, 4° S, 2° N, 8° N and 14° N, respectively.

(Left) Actual month of maximum monthly mean temperature is quite different due to inertia of atmosphere, land and ocean. It is July over the continents and August over the oceans in the NH, but its distribution is not simple.

Koppen climate classification

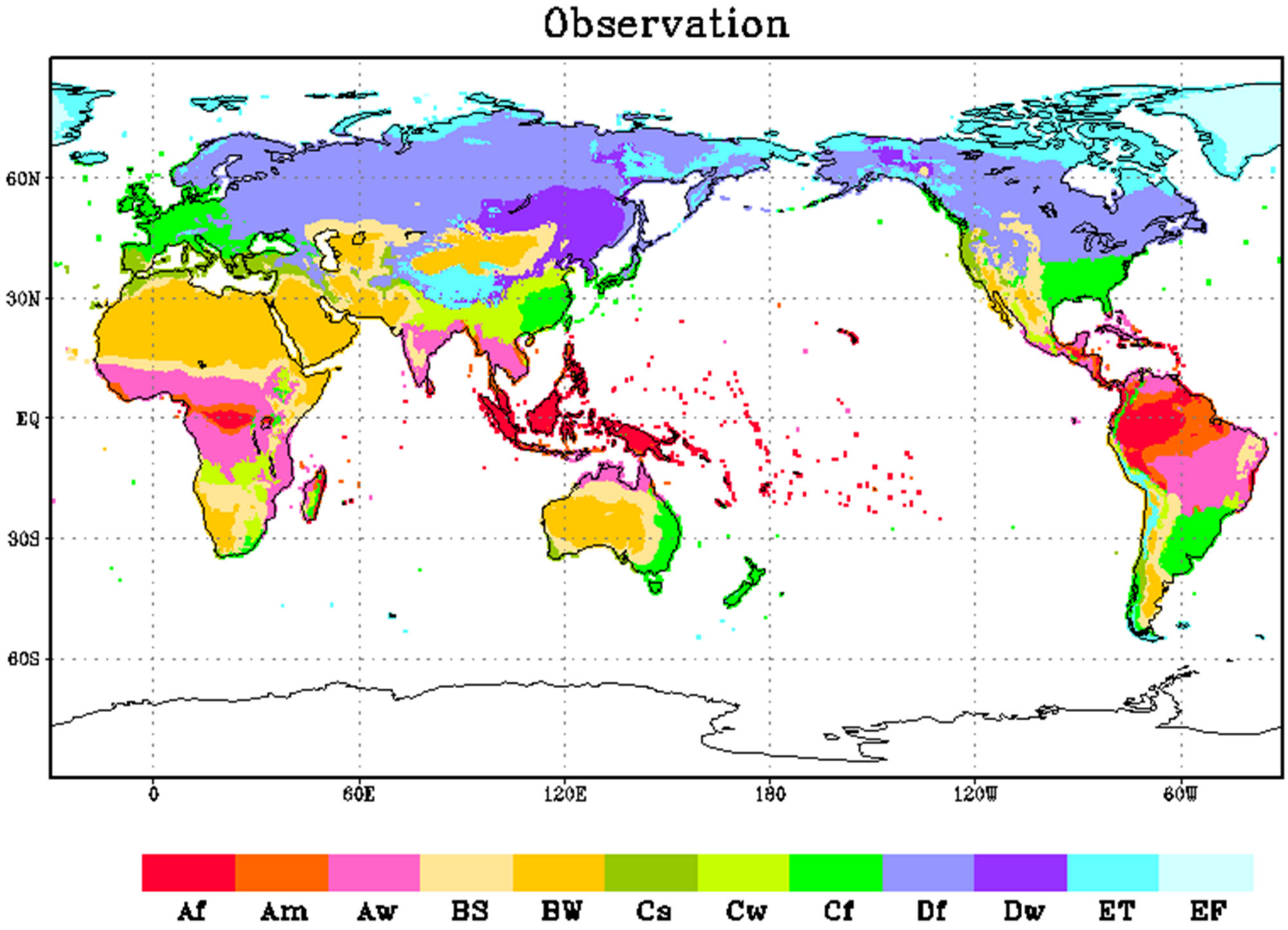

Climate Modeling

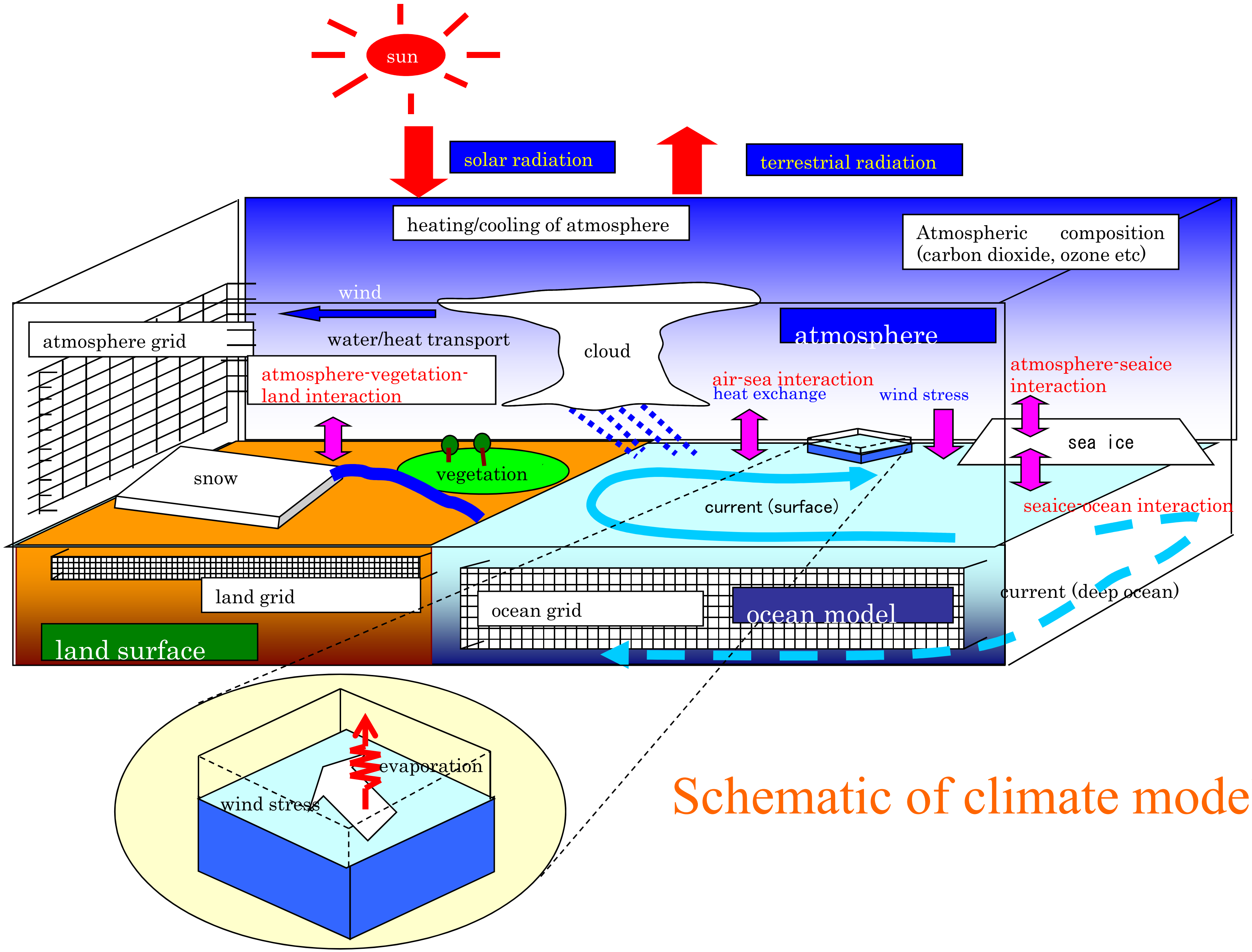

Schematic of climate model

MRI Coupled Atmosphere-Ocean General Circulation Model (MRI-CGCM2)

- AGCM
  - –MRI/JMA98
  - –T42 (2.8x2.8), L30 (top at 0.4 hPa)
  - –Longwave radiation - Shibata and Aoki (1989)
  - –Shortwave radiation - Shibata and Uchiyama (1992)
  - –Cumulus - Prognostic Arakawa-Schubert type
  - –PBL - Mellor and Yamada level 2 (1974)
  - –Land Surface - L3SiB or MRI/JMA_SiB
- OGCM
  - –Resolution : 2.5x(0.5-2.0), 23layers
  - –Eddy mixing : Isopycnal mixing, GM
  - –Seaice : Mellor and Kantha (1989)
- Coupling
  - –Time interval : 24hours
  - –Flux adjustment: used “with” or “without”

Obs

Model

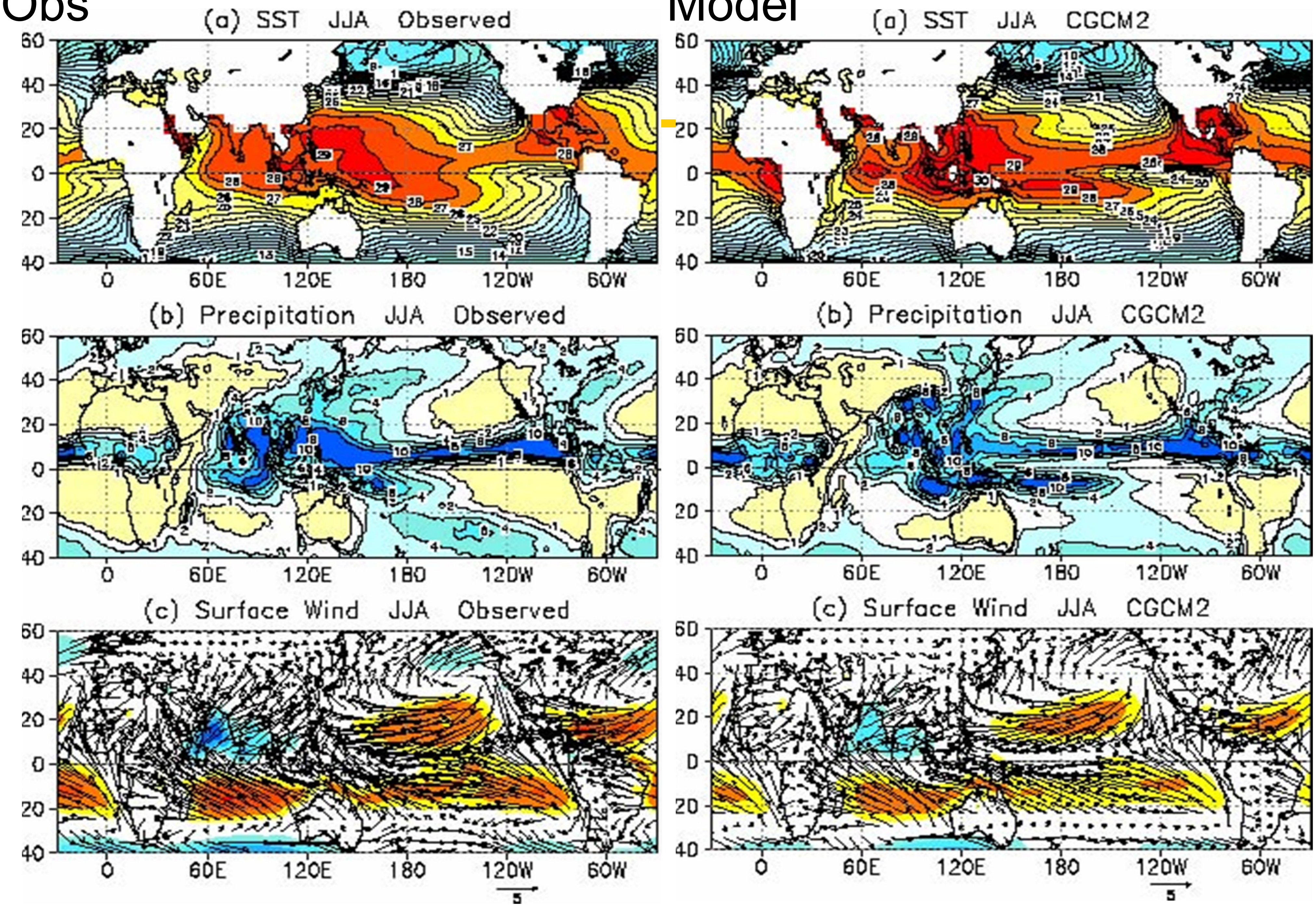
(a) SST JJA Observed
(b) Precipitation JJA Observed
(c) Surface Wind JJA Observed
(a) SST JJA CGCM2
(b) Precipitation JJA CGCM2
(c) Surface Wind JJA CGCM2
60
40
20
0
20
40
0
60E
120E
180
120W
60W
5

Onset Pentad: the Julian pentad in which the relative climatological pentad mean rainfall rate exceeds 4 mm/day.

Indian region

- **Northeastward progression over AS and the northwestward progression over the Bay of Bengal are well reproduced.**

East Asia

- **The model simulates earlier monsoon onset over southeast Asia.**
- **Onset over Indochina in early May, the mid-May onset over the SCS & later northward progression due to Meiyu/Baiu rainband are all simulated, although the precise timings differ slightly.**
- **In northern China, onset is earlier and precipitation is heavier.**

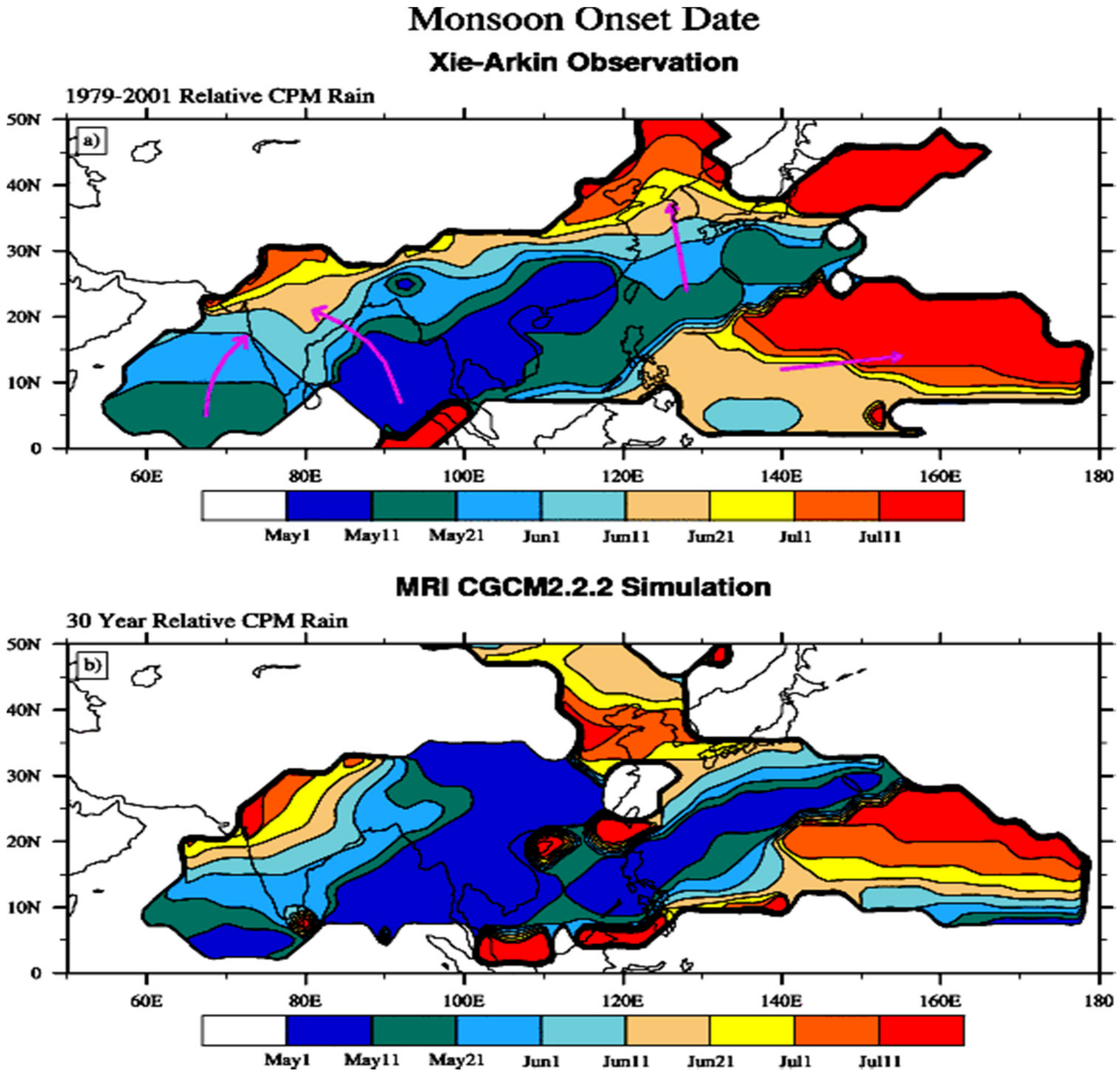

Mean Evolution of Monsoon: Withdrawal

Withdrawal Pentad: the transitional pentad in which rainfall drops below 4 mm/day.

Observation shows:

- southward retreat of monsoon over India, southeast Asia and Western north Pacific
- northward retreat over East Asia.

Simulation close to observation.

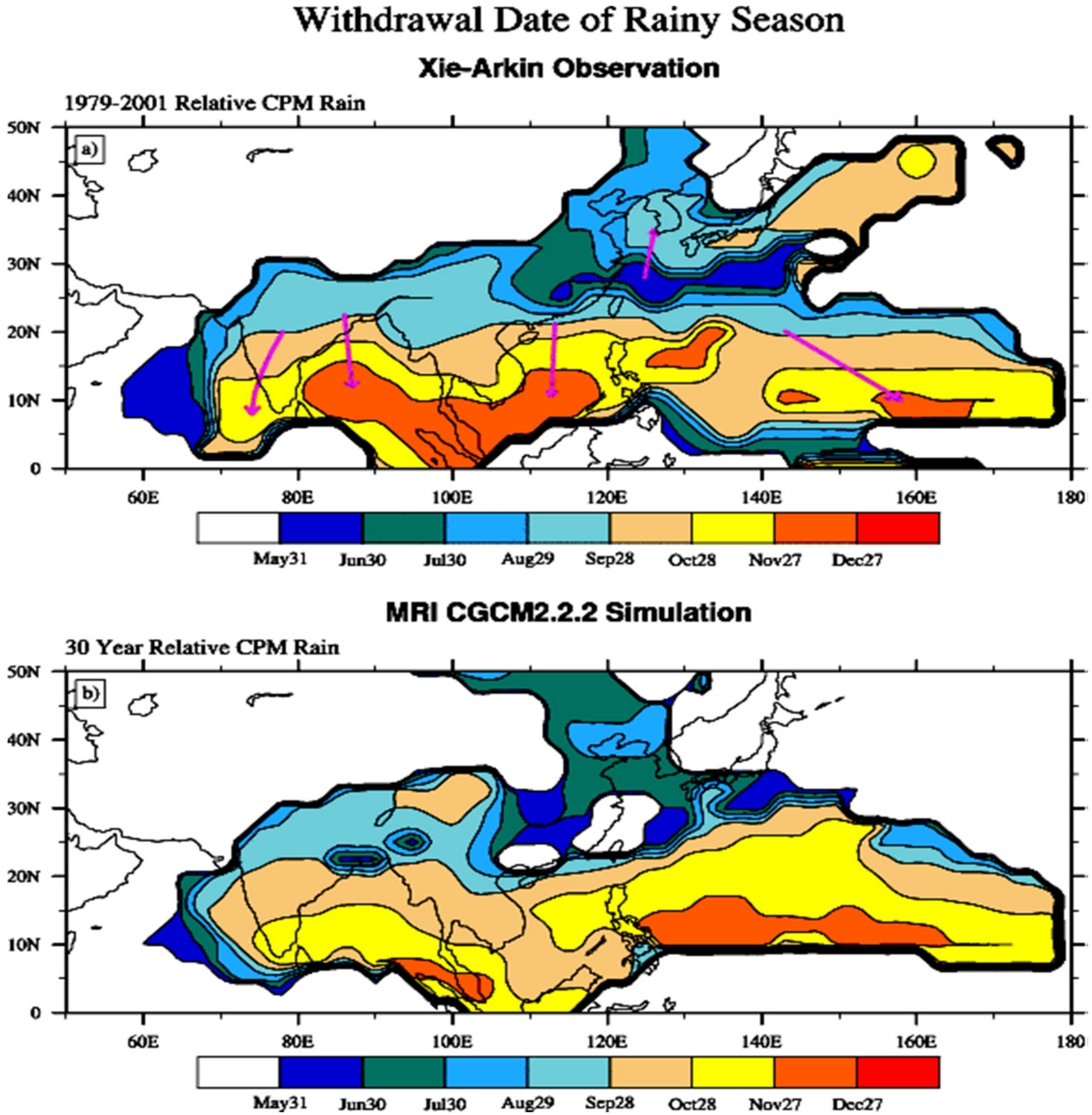

Role of orography on climate

Effect of mountains on climate

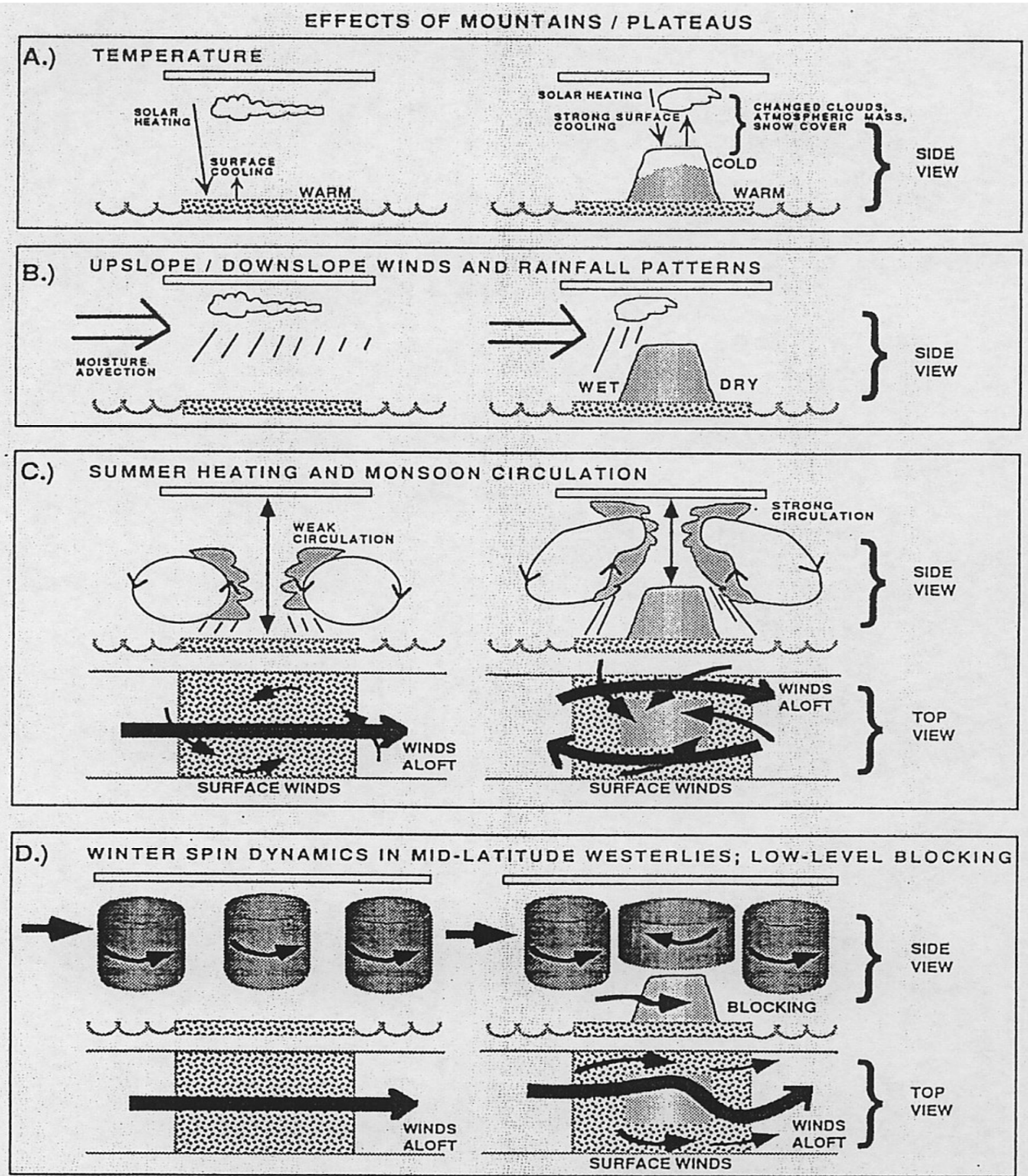

Figure 1. Effects of mountains/plateaus on climate: (*a*) temperature, (*b*) upslope/downslope winds and rainfall patterns, (*c*) summer heating and monsoon circulation, and (*d*) winter spin dynamics in mid-latitude westerlies, and low-level blocking. See text for explanation.

Kutzbach et al. (1993) J.Geology

Effect of mountain: Koppen climate

(Kitoh, 2005)

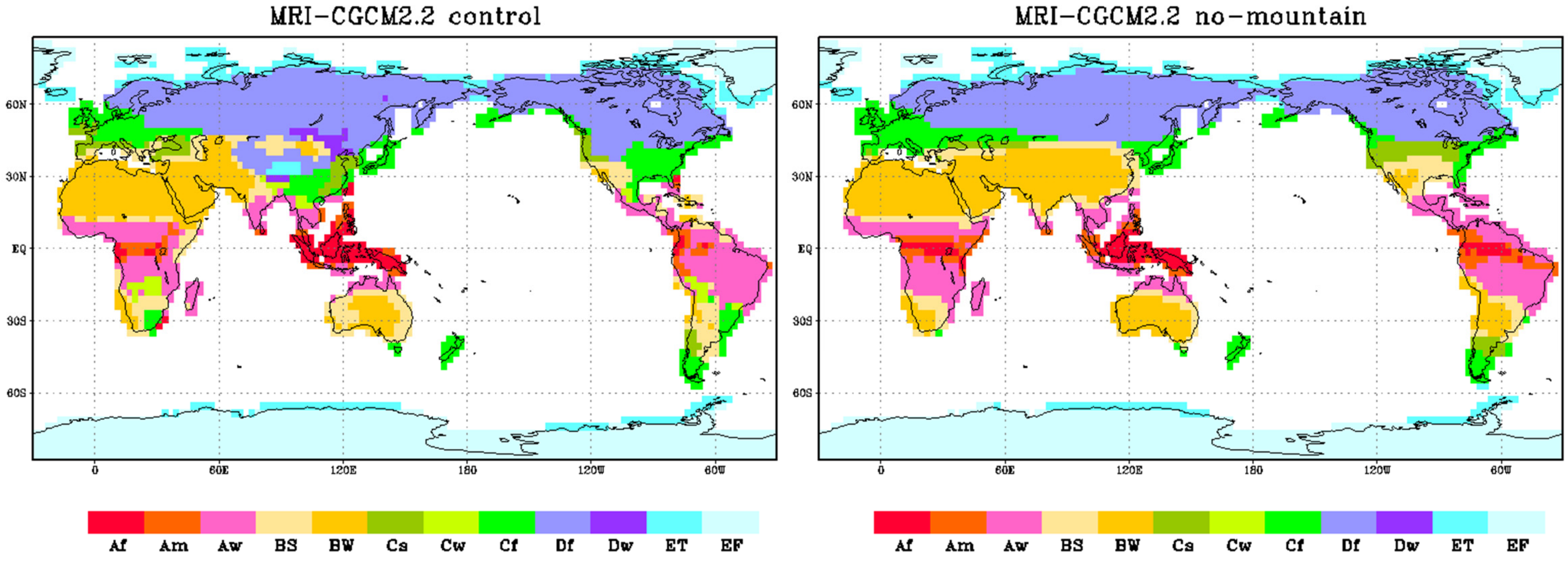

A: Tropical humid (Tropical wet, Tropical monsoonal, Tropical savanna)

B: Dry (Subtropical desert, Subtropical steppe, Mid-latitude desert, Mid-latitude steppe)

C: Mild mid-latitude (Mediterranean, Humid subtropical, Marine west coast)

D: Severe mid-latitude (Humid continental or Subarctic)

E: Polar (Tsundra, Ice cap)

Paleo climate

Orbital parameters

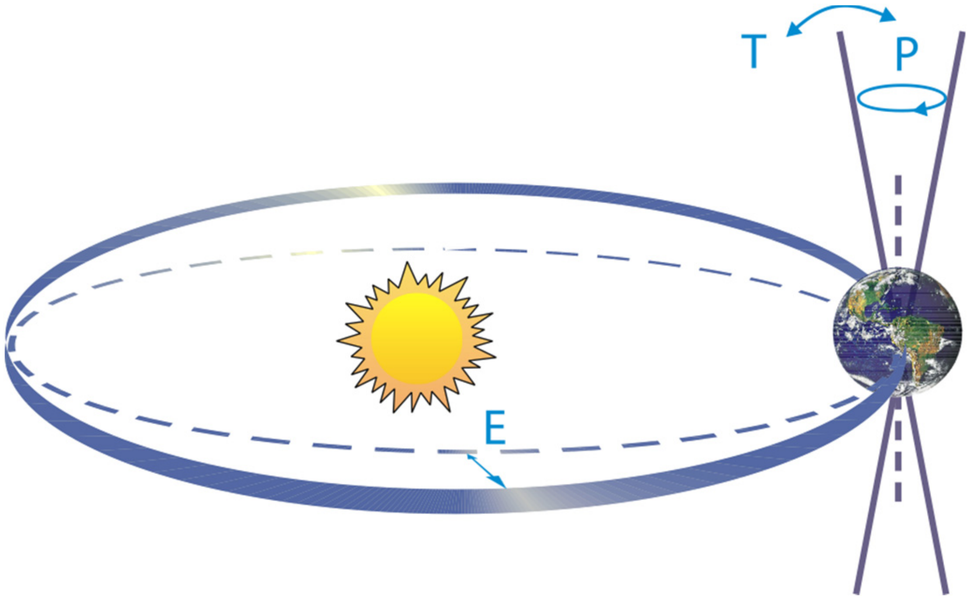

There are three fundamental ways the Earth's radiation balance can change, thereby causing a climate change:

(1) changing the incoming solar radiation (e.g., by changes in the Earth's orbit or in the Sun itself),

(2) changing the fraction of solar radiation that is reflected (this fraction is called the albedo – it can be changed, for example, by changes in cloud cover, small particles called aerosols or land cover), and

(3) altering the longwave energy radiated back to space (e.g., by changes in greenhouse gas concentrations).

(4) local climate also depends on how heat is distributed by winds and ocean currents.

Schematic of the Earth's orbital changes (Milankovitch cycles) that drive the ice age cycles. 'T' denotes changes in the tilt (or obliquity) of the Earth's axis, 'E' denotes changes in the eccentricity of the orbit (due to variations in the minor axis of the ellipse), and 'P' denotes precession, that is, changes in the direction of the axis tilt at a given point of the orbit. Source: Rahmstorf and Schellnhuber (2006).

Mid-Holocene: 6ka

Tassili n'Ajjer, Algeria
- Sahara was greener

Last Glacial Maximum: 21ka